Bose-Einstein and Fermi-Dirac distributions in nonextensive quantum statistics: Exact and interpolation approaches

Hideo Hasegawa*
Department of Physics, Tokyo Gakugei University, Koganei, Tokyo 184-8501, Japan
(Received 13 April 2009; revised manuscript received 24 June 2009; published 21 July 2009)

Generalized Bose-Einstein and Fermi-Dirac distributions in nonextensive quantum statistics have been discussed by the maximum-entropy method (MEM) with the optimum Lagrange multiplier based on the exact integral representation [A. K. Rajagopal, R. S. Mendes, and E. K. Lenzi, Phys. Rev. Lett. **80**, 3907 (1998)]. It has been shown that the $(q-1)$ expansion in the exact approach agrees with the result obtained by the asymptotic approach valid for $O(q-1)$. Model calculations have been made with a uniform density of states for electrons and with the Debye model for phonons. Based on the result of the exact approach, we have proposed the *interpolation approximation* to the generalized distributions, which yields results in agreement with the exact approach within $O(q-1)$ and in high- and low-temperature limits. By using the four methods of the exact, interpolation, factorization, and superstatistical approaches, we have calculated coefficients in the generalized Sommerfeld expansion and electronic and phonon specific heats at low temperatures. A comparison among the four methods has shown that the interpolation approximation is potentially useful in the nonextensive quantum statistics. Supplementary discussions have been made on the $(q-1)$ expansion of the generalized distributions based on the exact approach with the use of the un-normalized MEM, whose results also agree with those of the asymptotic approach.

DOI: 10.1103/PhysRevE.80.011126 PACS number(s): 05.30.−d, 05.70.Ce

I. INTRODUCTION

In the last decade, many studies have been made for the nonextensive statistics [1] in which the generalized entropy (the Tsallis entropy) is introduced (for a recent review, see [2]). The Tsallis entropy is a one-parameter generalization of the Boltzmann-Gibbs entropy with the entropic index q: the Tsallis entropy in the limit of $q=1.0$ reduces to the Boltzmann-Gibbs entropy. The optimum probability distribution or density matrix is obtained with the maximum-entropy method (MEM) for the Tsallis entropy with some constraints. At the moment, there are four possible MEMs: original method [1], un-normalized method [3], normalized method [4], and optimal Lagrange multiplier (OLM) method [5]. The four methods are equivalent in the sense that distributions derived in them are easily transformed to each other [6]. A comparison among the four MEMs is made in Ref. [2]. The nonextensive statistics has been successfully applied to a wide class of subjects in physics, chemistry, information science, biology, and economics [7].

One of the alternative approaches to the nonextensive statistics besides the MEM is the superstatistics [8,9] (for a recent review, see [10]). In the superstatistics, it is assumed that locally the equilibrium state is described by the Boltzmann-Gibbs statistics and that their global properties may be expressed by a superposition over the intensive parameter (i.e., the inverse temperature) [8–10]. It is, however, not clear how to obtain the mixing probability distribution of fluctuating parameter from first principles. This problem is currently controversial and some attempts to this direction have been proposed [11–15]. The concept of the superstatistics has been applied to many kinds of subjects such as hydrodynamic turbulence [16–18], cosmic ray [19], and solar flares [20].

The nonextensive statistics has been applied to both classical and quantum systems. In this paper, we pay attention to quantum nonextensive systems. The generalized Bose-Einstein and Fermi-Dirac distributions in nonextensive systems (referred to as q-BED and q-FDD hereafter) have been discussed by the three methods. (i) The asymptotic approximation (AA) was proposed by Tsallis *et al.* [21] who derived the expression for the canonical partition function valid for $|q-1|/k_BT \to 0$. It has been applied to the black-body radiation [21], early universe [21,22], and the Bose-Einstein condensation [21,23]. (ii) The factorization approximation (FA) was proposed by Büyükkilic *et al.* [24] to evaluate the grand-canonical partition function. The FA was criticized in [25,26] but supported in [27], related discussion being given in Sec. IV. The simple expressions for q-BED and q-FDD in the FA have been adopted in many applications such as the black-body radiation [23,28–30], early universe [31,32], the Bose-Einstein condensation [33–39], metals [40], superconductivity [41,42], spin systems [43–48], and metallic ferromagnets [49]. (iii) The exact approach (EA) was developed by Rajagopal and co-workers [50,51] who derived the formally exact integral representation for the grand-canonical partition function of nonextensive systems which is expressed in terms of the Boltzmann-Gibbs counterpart. The integral representation approach was originated from the Hilhorst formula [52]. Because an actual evaluation of a given integral is generally difficult, it may be performed in an approximate way [50,51] or in the limited cases [53]. The validity of the EA is discussed in [54,55]. The EA has been applied to nonextensive quantum systems such as black-body radiation [56,57] and the Bose-Einstein condensation [50,51].

We believe that it is important and valuable to pursue the EA despite its difficulty. It is the purpose of the present study

*hideohasegawa@goo.jp

to apply the EA [50,51] to calculations of the generalized distributions of q-BED and q-FDD. The grand-canonical partition function of the nonextensive systems is derived with the use of the OLM scheme in the MEM [5]. Self-consistent equations for averages of the number of particles and energy and the grand-canonical partition function are exactly expressed by the integral representation [50,51]. The integral representation for $q>1.0$ in the EA is expressed as an integral along the real axis, while that for $q<1.0$ is expressed as the contour integral in the complex plane [50,51,53]. We have shown that the $(q-1)$ expansion by the EA agrees with the result derived by the AA. For $q \geq 1.0$, the self-consistent equations have been numerically solved with the band model for electrons and the Debye model for phonon.

It is rather difficult and tedious to obtain the generalized distributions in the EA because they need the self-consistent calculation of averages of number of particles and energy. Based on the exact result obtained, we have proposed the *interpolation approximation* (IA) to q-BED and q-FDD, which do not need the self-consistently determined quantities and whose results are in agreement with those of the EA within $O(q-1)$ and in high- and low-temperature limits. We may obtain the simple analytic expressions of the q-BED and q-FDD.

The paper is organized as follows. In Sec. II, the exact integral representation is derived with the OLM-MEM after Ref. [50,51,53]. We have discussed the $(q-1)$ expansion of physical quantities using the EA and AA. Numerical calculations are performed for electron and phonon models for which we present the q-BED and q-FDD with the temperature-dependent energy. In Sec. III, we propose the IA in which analytical expressions for q-BED and q-FDD are obtained. In Sec. IV, a comparison is made between the generalized distributions calculated by the four methods of the EA, IA, FA [24], and superstatistical approximation (SA). A controversy on the validity of the FA [24] is discussed. With the use of the four methods, the generalized Sommerfeld expansion and low-temperature electronic and phonon specific heats are calculated. Section V is devoted to our conclusion. In Appendix A, we present a study of the EA and AA with the un-normalized MEM [3,21], calculating the $(q-1)$ expansion of the q-BED and q-FDD. Supplementary discussions on the IA are presented in Appendix B.

II. EXACT APPROACH

A. MEM by OLM

We will study nonextensive quantum systems described by the Hamiltonian $\hat{H}$. We have obtained the optimum density matrix of $\hat{\rho}$, applying the OLM-MEM to the Tsallis entropy given by [5,6]

$$S_q = \frac{k_B}{q-1}[1 - \mathrm{Tr}\ \hat{\rho}_q^q],$$

with the constraints

$$\mathrm{Tr}\ \hat{\rho}_q = 1,$$

$$\mathrm{Tr}\{\hat{\rho}_q^q N\} = c_q N_q,$$

$$\mathrm{Tr}\{\hat{\rho}_q^q H\} = c_q E_q,$$

$$c_q = \mathrm{Tr}\ \hat{\rho}_q^q,$$

where Tr stands for the trace, k_B is the Boltzmann constant, and E_q and N_q denote the expectation values of the Hamiltonian $\hat{H}$ and the number operator $\hat{N}$, respectively. The OLM-MEM yields [5,6]

$$\hat{\rho}_q = \frac{1}{X_q}[1 + (q-1)\beta(\hat{H} - \mu\hat{N} - E_q + \mu N_q)]^{1/(1-q)}, \quad (1)$$

$$X_q = \mathrm{Tr}\{[1 + (q-1)\beta(\hat{H} - \mu\hat{N} - E_q + \mu N_q)]^{1/(1-q)}\}, \quad (2)$$

$$N_q = \frac{1}{X_q}\mathrm{Tr}\{[1 + (q-1)\beta(\hat{H} - \mu\hat{N} - E_q + \mu N_q)]^{q/(1-q)}\hat{N}\}, \quad (3)$$

$$E_q = \frac{1}{X_q}\mathrm{Tr}\{[1 + (q-1)\beta(\hat{H} - \mu\hat{N} - E_q + \mu N_q)]^{q/(1-q)}\hat{H}\}, \quad (4)$$

where β and μ denote the Lagrange multipliers. In deriving Eqs. (1)–(4), we have employed the relation

$$c_q = X_q^{1-q}.$$

Lagrange multipliers of β and μ are identified as the inverse physical temperature ($\beta = 1/k_B T$) and the chemical potential (Fermi level), respectively [5,6].

B. Exact integral representation

1. Case of $q>1$

In the case of $q>1.0$, we adopt the formula for the gamma function $\Gamma(s)$,

$$x^{-s} = \frac{1}{\Gamma(s)}\int_0^\infty u^{s-1}e^{-xu}du \quad \text{for Re } s > 0. \quad (5)$$

With $s=1/(q-1)$ [or $s=q/(q-1)$] and $x=1+(q-1)\beta(H-\mu N)$ in Eq. (5), we may express Eqs. (1)–(4) by [50,51]

$$N_q = \frac{1}{X_q}\int_0^\infty G\left(u;\frac{q}{q-1},1\right)e^{(q-1)\beta u(E_q-\mu N_q)} \times \Xi_1[(q-1)\beta u]N_1[(q-1)\beta u]du, \quad (6)$$

$$E_q = \frac{1}{X_q}\int_0^\infty G\left(u;\frac{q}{q-1},1\right)e^{(q-1)\beta u(E_q-\mu N_q)}\Xi_1[(q-1)\beta u] \times E_1[(q-1)\beta u]du, \quad (7)$$

with

$$X_q = \int_0^\infty G\left(u;\frac{1}{q-1},1\right)e^{(q-1)\beta u(E_q-\mu N_q)}\Xi_1[(q-1)\beta u]du, \tag{8}$$

where

$$\Xi_1(u) = e^{-u\Omega_1(u)} = \mathrm{Tr}\{e^{-u(\hat{H}-\mu\hat{N})}\} = \prod_k [1 \mp e^{-u(\epsilon_k-\mu)}]^{\mp 1}, \tag{9}$$

$$\Omega_1(u) = \pm\frac{1}{u}\sum_k \ln[1 \mp e^{-u(\epsilon_k-\mu)}], \tag{10}$$

$$N_1(u) = \sum_k f_1(\epsilon_k,u), \tag{11}$$

$$E_1(u) = \sum_k \epsilon_k f_1(\epsilon_k,u), \tag{12}$$

$$f_1(\epsilon,u) = \frac{1}{e^{u(\epsilon-\mu)} \mp 1}, \tag{13}$$

$$G(u;a,b) = \frac{b^a}{\Gamma(a)}u^{a-1}e^{-bu}. \tag{14}$$

The upper (lower) sign in Eqs. (9), (10), and (13) denotes boson (fermion) case, and $\Xi_1(u)$, $\Omega_1(u)$, $N_1(u)$, $E_1(u)$, and $f_1(\epsilon,u)$ express the physical quantities for $q=1.0$. Equations (6)–(8) show that physical quantities in nonextensive systems are expressed as a superposition of those for $q=1.0$.

Although Eqs. (6)–(8) are formally exact expressions, they have a problem when we perform numerical calculations. The gamma distribution of $G[u;1/(q-1)+\ell,1]$ $(\ell=0,1)$ in Eqs. (6)–(8) has the maximum at u_{max} and it has average and variance given by

$$u_{max} = \frac{1}{(q-1)} + \ell - 1, \tag{15}$$

$$\langle u\rangle_u = \frac{1}{(q-1)} + \ell, \tag{16}$$

$$\langle u^2\rangle_u - \langle u\rangle_u^2 = \frac{1}{(q-1)} + \ell. \tag{17}$$

Equation (15) shows that the gamma distribution in Eqs. (6)–(8) has the maximum at $u_{max}=1/(q-1)\to\infty$, while the contribution from $\Xi_1[(q-1)\beta t]$ is dominant at $t\sim 0$ because its argument becomes $(q-1)\beta t\to 0$. Then numerical calculations using Eqs. (6)–(8) are very difficult.

In order to overcome this difficulty, we have adopted a change in variable $(q-1)\beta u\to u$ in Eq. (6)–(8) to obtain alternative expressions given by

$$N_q = \frac{1}{X_q}\int_0^\infty G\left(u;\frac{1}{q-1}+1,\frac{1}{(q-1)\beta}\right) \times e^{u(E_q-\mu N_q)}\Xi_1(u)N_1(u)du, \tag{18}$$

$$E_q = \frac{1}{X_q}\int_0^\infty G\left(u;\frac{1}{q-1}+1,\frac{1}{(q-1)\beta}\right) \times e^{u(E_q-\mu N_q)}\Xi_1(u)E_1(u)du, \tag{19}$$

with

$$X_q = \int_0^\infty G\left(u;\frac{1}{q-1},\frac{1}{(q-1)\beta}\right)e^{u(E_q-\mu N_q)}\Xi_1(u)du. \tag{20}$$

The gamma distribution of $G(u;\frac{1}{(q-1)}+\ell,\frac{1}{(q-1)\beta})$ for $\ell=0,1$ in Eqs. (18)–(20) has the maximum at u_{max} and it has average, mean square, and variance given by

$$u_{max} = [1+(q-1)(\ell-1)]\beta, \tag{21}$$

$$\langle u\rangle_u = [1+(q-1)\ell]\beta, \tag{22}$$

$$\langle u^2\rangle_u = [1+(q-1)\ell][1+(q-1)(\ell+1)]\beta^2, \tag{23}$$

$$\langle u^2\rangle_u - \langle u\rangle_u^2 = (q-1)[1+(q-1)\ell]\beta^2. \tag{24}$$

Equation (21) shows that the gamma distribution has the maximum at $u_{max}=\beta$ in the limit of $q\to 1.0$, and an integration over u in Eqs. (18)–(20) may be easily performed. Indeed, in the case of $q\gtrsim 1.0$ discussed above, the gamma distribution in Eqs. (18)–(20) becomes

$$G\left(u;\frac{1}{q-1}+\ell,\frac{1}{(q-1)\beta}\right) = \begin{cases} \dfrac{1}{\sqrt{2\pi(q-1)\beta^2}}e^{-\{1/[2(q-1)\beta^2]\}(u-\beta)^2} & \text{for } (q-1)\beta^2 \ll 1, \quad (25) \\ \delta(u-\beta) & \text{for } (q-1)\beta^2 \to 0. \quad (26) \end{cases}$$

Although expressions given by Eqs. (6)–(8) are mathematically equivalent to those given by Eqs. (18)–(20), the latter expressions are more suitable than the former ones for numerical calculations.

2. Case of $q<1$

In the case of $q<1.0$, we adopt the formula that is given by

$$x^s = \frac{i}{2\pi}\Gamma(s+1)\int_C (-t)^{-s-1}e^{-xt}dt \quad \text{for Re } s > 0, \quad (27)$$

where a contour integral is performed over the Hankel path C in the complex plane. With $s=1/(1-q)$ [or $s=q/(1-q)$] and $x=1+(q-1)\beta(H-\mu N)$ in Eq. (27), we obtain [50,51]

$$N_q = \frac{i}{2\pi X_q}\int_C H\left(t;\frac{q}{1-q},1\right)e^{-(1-q)\beta t(E_q-\mu N_q)} \times \Xi_1[-(1-q)\beta t]N_1[-(1-q)\beta t]dt, \quad (28)$$

$$E_q = \frac{i}{2\pi X_q}\int_C H\left(t;\frac{q}{1-q},1\right)e^{-(1-q)\beta t(E_q-\mu N_q)} \times \Xi_1[-(1-q)\beta t]E_1[-(1-q)\beta t]dt, \quad (29)$$

with

$$X_q = \frac{i}{2\pi}\int_C H\left(t;\frac{1}{1-q},1\right)e^{-(1-q)\beta t(E_q-\mu N_q)}\Xi_1[-(1-q)\beta t]dt, \quad (30)$$

$$H(t;a,b) = \Gamma(a+1)b^{-a}(-t)^{-a-1}e^{-bt}, \quad (31)$$

where $\Xi_1(u)$, $N_1(u)$, $E_1(u)$, and $f_1(\epsilon,u)$ are given by Eqs. (9)–(12) with complex u.

In the case of $q<1.0$, N_q, E_q, and X_q given by Eqs. (28)–(30) are expressed by an integral along the Hankel contour path C in the complex plane. The Hankel path may be modified to the Bromwich contour which is parallel to the imaginary axis from $c-i\infty$ to $c+i\infty$ $(c>0)$ [56,57]. The Bromwich contour is usually understood as counting the contributions from the residues of all poles located in the left side of Re $z<c$ of the complex plane z when the integrand is expressed by simple analytic functions. If the integrand is not expressed by simple analytic functions, we have to evaluate it by numerical methods. Unfortunately, we have not succeeded in evaluating Eqs. (28)–(30) with the sufficient accuracy. It is not easy to numerically evaluate the integral along the Hankel or Bromwich contour, which is required to be appropriately deformed for actual numerical calculations [58,59]. This subject has a long history and it is still active in the field of the numerical methods for the inverse Laplace transformation [58] and for the gamma functions [59].

It is worthwhile to remark that for a Bose gas model with the density of states of $\rho(\epsilon)=A\epsilon^r$, we obtain (with $\mu=0$) [52,56,57]

$$\Xi_1(u) = \exp\left[\frac{A\Gamma(r+1)\zeta(r+2)}{u^{r+1}}\right],$$

$$N_1(u) = \frac{A\Gamma(r+1)\zeta(r+1)}{u^{r+1}},$$

$$E_1(u) = \frac{A\Gamma(r+2)\zeta(r+2)}{u^{r+2}},$$

where $r=1/2$ for an ideal Bose gas, $r=2$ for a harmonic oscillator, A denotes a relevant factor, and $\zeta(z)$ stands for the Riemann zeta function. With a repeated use of Eq. (27), N_q, E_q, and X_q may be expressed as sums of gamma functions [52,56,57]. Unfortunately, such a sophisticated method cannot be necessarily applied to any models such as Fermi gas.

With a change in variable of $(1-q)\beta(-t)\to(-t)$ in Eqs. (28)–(30) after the case of $q>1$, they are given by

$$N_q = \frac{i}{2\pi X_q}\int_C H\left(t;\frac{1}{1-q}-1,\frac{1}{(1-q)\beta}\right) \times e^{-t(E_q-\mu N_q)}\Xi_1(-t)N_1(-t)dt, \quad (32)$$

$$E_q = \frac{i}{2\pi X_q}\int_C H\left(t;\frac{1}{1-q}-1,\frac{1}{(1-q)\beta}\right) \times e^{-t(E_q-\mu N_q)}\Xi_1(-t)E_1(-t)dt, \quad (33)$$

with

$$X_q = \frac{i}{2\pi}\int_C H\left(t;\frac{1}{1-q},\frac{1}{(1-q)\beta}\right)e^{-t(E_q-\mu N_q)}\Xi_1(-t)dt. \quad (34)$$

Average and mean square over $H(t,\frac{1}{1-q}-\ell,\frac{1}{(1-q)\beta})$ for $\ell=0,1$ are given by

$$\langle(-t)\rangle_t = [1-(1-q)\ell]\beta, \quad (35)$$

$$\langle(-t)^2\rangle_t = [1-(1-q)\ell][q-(1-q)\ell]\beta^2. \quad (36)$$

Equations (32)–(34) are useful in making the $(q-1)$ expansion, as will be discussed in the following.

C. $(q-1)$ expansion

1. Exact approach

We will consider the $(q-1)$ expansion of the expectation value of an operator $\hat{O}$ in the EA. By using Eqs. (18) and (32), we obtain

$$\langle\hat{O}\rangle_q = \frac{1}{X_q}\mathrm{Tr}\{[1-(1-q)\beta\hat{K}]^{q/(1-q)}\hat{O}\}, \quad (37)$$

$$\langle \hat{O} \rangle_q = = \begin{cases} \dfrac{1}{X_q} \displaystyle\int_0^\infty G\left(u; \frac{q}{q-1}, \frac{1}{(q-1)\beta}\right) Y_1(u) O_1(u) du & \text{for } q > 1, \quad (38) \\ \dfrac{i}{2\pi X_q} \displaystyle\int_C H\left(t; \frac{q}{1-q}, \frac{1}{(1-q)\beta}\right) Y_1(-t) O_1(-t) dt & \text{for } q < 1, \quad (39) \end{cases}$$

with

$$O_1(u) = \frac{\mathrm{Tr}\{e^{-u\hat{K}}\hat{O}\}}{Y_1(u)}, \quad (40)$$

$$Y_1(u) = \mathrm{Tr}\{e^{-u\hat{K}}\} = e^{u(E_q - \mu N_q)} \Xi_1(u), \quad (41)$$

$$\hat{K} = \hat{H} - \mu\hat{N} - E_q + \mu N_q, \quad (42)$$

where X_q is given by Eq. (20) for $q>1$ and by Eq. (34) for $q<1$. It is noted that $Y_1(u)$ includes the self-consistently calculated N_q and E_q.

We first consider the case of $q \gtrsim 1$ for which the integral including an arbitrary function $W(u)$ is assumed to be given by

$$J = \int_0^\infty G\left(u; \frac{1}{q-1} + \ell, \frac{1}{(q-1)\beta}\right) W(u) du \quad \text{for } \ell = 0, 1. \quad (43)$$

Since $G(u; \frac{1}{q-1}+\ell, \frac{1}{(q-1)\beta})$ has the maximum around $u=\beta$ as mentioned before [Eq. (21)], $W(u)$ may be expanded as

$$W(u) = W(\beta) + (u-\beta)\frac{\partial W}{\partial \beta} + \frac{1}{2}(u-\beta)^2 \frac{\partial^2 W}{\partial \beta^2} + \cdots. \quad (44)$$

Substituting Eq. (44) to Eq. (43) and using the relations given by Eqs. (22) and (23), we obtain J in a series of $(q-1)$ as

$$J = W(\beta) + \langle (u-\beta) \rangle_u \frac{\partial W}{\partial \beta} + \frac{1}{2}\langle (u-\beta)^2 \rangle_u \frac{\partial^2 W}{\partial \beta^2} + \cdots, \quad (45)$$

$$J = W(\beta) + (q-1)\left[\ell\beta\frac{\partial W}{\partial \beta} + \frac{1}{2}\beta^2 \frac{\partial^2 W}{\partial \beta^2}\right] + \cdots \quad \text{for } q \simeq 1.0. \quad (46)$$

Next we consider the case of $q \lesssim 1$ for which a similar integral along the Hankel path C is given by

$$J = \frac{i}{2\pi}\int_C H\left(t; \frac{q}{1-q} - \ell, \frac{1}{(1-q)\beta}\right) W(-t) dt \quad \text{for } \ell = 0, 1. \quad (47)$$

By expanding $W(-t)$ at $-t=\beta$ and using the relations for averages given by Eqs. (35) and (36), we obtain the same expression for J as Eq. (46), which is then valid both for $q \lesssim 1.0$ and $q \gtrsim 1.0$.

For $W(u)=Y_1(u)$ and $W(u)=Y_1(u)O_1(u)$ in Eq. (46), we obtain

$$X_q = Y_1 + \frac{1}{2}(q-1)\beta^2 \frac{\partial^2 Y_1}{\partial \beta^2} + \cdots, \quad (48)$$

$$O_q = \frac{1}{X_q}\left[Y_1 O_1 + (q-1)\beta\frac{\partial (Y_1 O_1)}{\partial \beta} + \frac{1}{2}(q-1)\beta^2 \frac{\partial^2 (Y_1 O_1)}{\partial \beta^2} + \cdots \right]. \quad (49)$$

Note that the $O[(q-1)\beta]$ term in Eq. (48) vanishes because $\ell=0$ in Eq. (46). Substituting the relations given by

$$\frac{\partial Y_1}{\partial \beta} = -\langle \hat{K} \rangle_1 Y_1, \quad (50)$$

$$\frac{\partial^2 Y_1}{\partial \beta^2} = \langle \hat{K}^2 \rangle_1 Y_1, \quad (51)$$

$$\frac{\partial O_1}{\partial \beta} = \langle \hat{K} \rangle_1 \langle \hat{O} \rangle_1 - \langle \hat{K}\hat{O} \rangle_1, \quad (52)$$

$$\frac{\partial^2 O_1}{\partial \beta^2} = \langle \hat{K}^2 \hat{O} \rangle_1 - \langle \hat{K}^2 \rangle_1 \langle \hat{O} \rangle_1 + 2[\langle \hat{K} \rangle_1 \langle \hat{K}\hat{O} \rangle_1 - \langle \hat{K} \rangle_1^2 \langle \hat{O} \rangle_1] \quad (53)$$

to Eqs. (48) and (49), we finally obtain the $O(q-1)$ expansion of O_q given by

$$O_q \simeq O_1 + (1-q)\left(\beta\langle \hat{K}\hat{O} \rangle_1 + \tfrac{1}{2}\beta^2[\langle \hat{K}^2 \rangle_1 \langle \hat{O} \rangle_1 - \langle \hat{K}^2 \hat{O} \rangle_1]\right) + \cdots. \quad (54)$$

2. Asymptotic approach

On the other hand, we may adopt the AA [21] to obtain O_q given by Eq. (37) valid for $O(q-1)$. By using the relation $e_q^x \simeq e^x[1-(1-q)x^2/2+\cdots]$ in Eqs. (2) and (37), we may expand X_q and O_q up to $O(q-1)$ as

$$X_q \simeq X_1\left[1 - \tfrac{1}{2}(1-q)\beta^2 \langle \hat{K}^2 \rangle_1 + \cdots\right], \quad (55)$$

$$O_q = \frac{1}{X_q}\mathrm{Tr}\{[1-(1-q)\beta\hat{K}]^{-1}[1-(1-q)\beta\hat{K}]^{1/(1-q)}\hat{O}\} \quad (56)$$

$$\simeq \frac{1}{X_q}\mathrm{Tr}\left\{e^{-\beta\hat{K}}[1+(1-q)\beta\hat{K}]\left[1-\frac{1}{2}(1-q)\beta^2\hat{K}^2\right]\hat{O}\right\} + \cdots \tag{57}$$

$$\simeq O_1 + (1-q)\left(\beta\langle\hat{K}\hat{O}\rangle_1 + \tfrac{1}{2}\beta^2[\langle\hat{K}^2\rangle_1\langle\hat{O}\rangle_1 - \langle\hat{K}^2\hat{O}\rangle_1]\right) + \cdots. \tag{58}$$

Equation (58) agrees with Eq. (54) obtained by the EA within $O(q-1)$. In Appendix A, we have shown that the same equivalence holds between the AA and EA with the un-normalized MEM [3,21].

D. Generalized distributions

1. $O(q-1)$ expansion

Equations for N_q and E_q given by Eqs. (18), (19), (32), and (33) may be expressed as

$$N_q = \sum_k f_q(\epsilon_k,\beta) = \int f_q(\epsilon,\beta)\rho(\epsilon)d\epsilon, \tag{59}$$

$$E_q = \sum_k f_q(\epsilon_k,\beta)\epsilon_k = \int f_q(\epsilon,\beta)\epsilon\rho(\epsilon)d\epsilon, \tag{60}$$

where $f_q(\epsilon,\beta)$ $[\equiv f_q(\epsilon)]$ signifies the generalized distributions, q-BED and q-FDD, given by

$$f_q(\epsilon,\beta) = \begin{cases} \dfrac{1}{X_q}\displaystyle\int_0^\infty G\left(u;\frac{q}{q-1},\frac{1}{(q-1)\beta}\right)Y_1(u)f_1(\epsilon,u)du & \text{for } q>1, \quad (61)\\ \dfrac{i}{2\pi X_q}\displaystyle\int_C H\left(t;\frac{q}{1-q},\frac{1}{(1-q)\beta}\right)Y_1(-t)f_1(\epsilon,-t)dt & \text{for } q<1, \quad (62)\end{cases}$$

with the density of states $\rho(\epsilon)$ given by

$$\rho(\epsilon) = \sum_k \delta(\epsilon-\epsilon_k). \tag{63}$$

In order to examine the $(q-1)$ expansion of the generalized distributions, we set $\hat{O}=\hat{n}_k$ in Eq. (54), where $\hat{n}_k$ denotes the number operator of the state k. A simple calculation leads to the $O(q-1)$ expansion of the generalized distribution given by

$$f_q(\epsilon,\beta) = f_1(\epsilon,\beta) + (q-1)\left[\beta\frac{\partial f_1}{\partial\beta} + \frac{1}{2}\beta^2\frac{\partial^2 f_1}{\partial\beta^2}\right] + \cdots \tag{64}$$

$$= f_1(\epsilon,\beta) + (q-1)\left[(\epsilon-\mu)\frac{\partial f_1}{\partial\epsilon} + \frac{1}{2}(\epsilon-\mu)^2\frac{\partial^2 f_1}{\partial\epsilon^2}\right] + \cdots. \tag{65}$$

In deriving Eq. (65), we have employed the relation $(\partial Y_1/\partial\beta)/Y_1(\beta) = -\langle H-\mu N\rangle_1 + (N_q-\mu N_q) \simeq O(q-1)$. In Appendix A, we have made a similar analysis with the un-normalized MEM, showing that Eq. (65) is consistent with Eq. (A39) which agrees with the result in the AA [21].

2. Properties of the generalized distribution

We will examine some limiting cases of the generalized distribution given by Eqs. (61) and (62).

(1) In the limit of $q\to 1.0$, Eq. (65) leads to

$$f_q(\epsilon,\beta) = f_1(\epsilon,\beta). \tag{66}$$

(2) In the zero-temperature limit of $T=0$, the q-FDD becomes

$$f_q(\epsilon,T=0) = \Theta(\mu-\epsilon) = f_1(\epsilon,T=0), \tag{67}$$

where $\Theta(x)$ stands for the Heaviside function. Equation (67) implies that the ground-state FD distribution is not modified by the nonextensivity.

(3) In the high-temperature limit of $\beta\to 0.0$, where $\Omega_1 \simeq -(1/\beta)\Sigma_k e^{-\beta(\epsilon_k-\mu)}$ with $\ln(1\pm x)\simeq \mp x$ for small x, we obtain $(\mu=0.0)$

$$f_q(\epsilon,\beta\to 0) \propto [1+(q-1)\beta(\epsilon-E_q)]^{[1/(1-q)]-1} = [e_q^{-\beta(\epsilon-\mu)}]^q, \tag{68}$$

e_q^x expressing the q-exponential function defined by

$$e_q^x = \exp_q(x) = \begin{cases}[1+(1-q)x]^{1/(1-q)} & \text{for } 1+(1-q)x>0, \quad (69)\\ 0 & \text{for } 1+(1-q)x\le 0, \quad (70)\end{cases}$$

with the cutoff properties. Equation (68) corresponds to the escort distribution,

$$P_q(\epsilon) = \frac{p_q(\epsilon)^q}{c_q} \propto [e_q^{-\beta(\epsilon-\mu)}]^q, \tag{71}$$

with the q-exponential distribution $p_q(\epsilon)$ given by

$$p_q(\epsilon) = e_q^{-\beta(\epsilon-\mu)}. \tag{72}$$

Equations (61) and (62) show that the ϵ dependence of $f_q(\epsilon,\beta)$ arises from that of $f_1(\epsilon,\beta)$. In particular, the q-FDD preserves the same ϵ symmetry as $f_1(\epsilon,\beta)$:

(a) $f_q(\epsilon,\beta)=1/2$ for $\epsilon=\mu$,

(b) $f_q(\epsilon,\beta)$ has the *antisymmetry*

$$f_q(-\delta\epsilon+\mu,\beta) - \tfrac{1}{2} = \tfrac{1}{2} - f_q(\delta\epsilon+\mu,\beta) \quad \text{for } \delta\epsilon>0,$$

(c) $\partial f_q(\epsilon,\beta)/\partial\epsilon$ is symmetric with respect to $\epsilon=\mu$.

E. Numerical calculations

1. Model for electrons

For model calculations of electron systems, we employ a uniform density of state given by

$$\rho(\epsilon) = (1/2W)\Theta(W - |\epsilon|), \tag{73}$$

where W denotes a half of the total bandwidth. We have performed numerical calculations of E_q and μ for $q \geq 1.0$ as a function of T for a given number of particles of N and the density of states $\rho(\epsilon)$. We may obtain analytical expressions for $\Xi_1(u)$, $N_1(u)$, and $E_1(u)$ which are necessary for our numerical calculations. By using Eq. (73) for Eqs. (9)–(12), we obtain (with $W=1.0$)

$$\Xi_1(u) = e^{-u\Omega_1(u)},$$

$$\Omega_1(u) = -\frac{1}{2u}\{\ln[1 + e^{-u(1-\mu)}] - \ln[1 + e^{-u(1+\mu)}] + \ln[1 + e^{u(1+\mu)}] - \ln[1 + e^{u(1-\mu)}]\} - \frac{1}{2u^2}\{Li_2(-e^{-u(1+\mu)}) - Li_2(-e^{u(1-\mu)})\},$$

$$N_1(u) = 1 + \frac{1}{2u}[\ln(1 + e^{-u(1+\mu)}) - \ln(1 + e^{u(1-\mu)})],$$

$$E_1(u) = -\frac{1}{2u}[\ln(1 + e^{-u(1+\mu)}) + \ln(1 + e^{u(1-\mu)})] + \frac{1}{2u^2}[Li_2(-e^{-u(1+\mu)}) - Li_2(-e^{u(1-\mu)})],$$

where $Li_n(z)$ denotes the nth polylogarithmic function defined by

$$Li_n(z) = \sum_{k=1}^{\infty} \frac{z^k}{k^n}.$$

We adopt $N=0.5$, for which $\mu=0.0$ independent of the temperature because of the adopted uniform density of states given by Eq. (73). The temperature dependence of E_q calculated self-consistently from Eqs. (18)–(20), is shown in Fig. 1 whose inset shows the enlarged plot for low temperatures ($k_BT/W \lesssim 0.1$). We note that E_q at low temperatures is larger for larger q although this trend is reversed at higher temperatures ($k_BT \gtrsim 0.3$).

The calculated q-FDDs $f_q(\epsilon)$ for various q values for $k_BT/W=0.1$ are shown in Figs. 2(a) and 2(b) whose ordinates are in the linear and logarithmic scales, respectively. It is shown that with more increasing q from unity, $f_q(\epsilon)$ at $\epsilon \gg \mu$ has a longer tail. The properties of $f_q(\epsilon)$ are more clearly seen in its derivative of $-\partial f_q(\epsilon)/\partial\epsilon$, which is plotted in Fig. 3 with the logarithmic ordinate. We note that $-\partial f_q(\epsilon)/\partial\epsilon$ is symmetric with respect of $\epsilon=\mu$. With increasing q above unity, $-\partial f_q(\epsilon)/\partial\epsilon$ has a longer tail. Dotted and solid curves for $q<1.0$ in Figs. 2 and 3 will be discussed in Sec. III C.

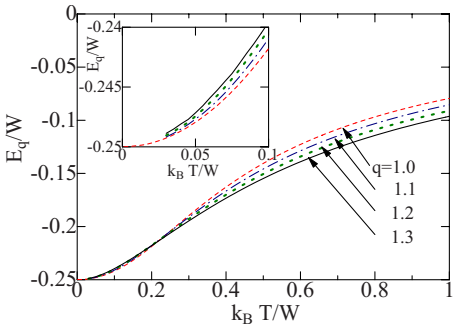

FIG. 1. (Color online) The temperature dependence of E_q of the electron model for $q=1.0$ (dashed curves), $q=1.1$ (chain curves), $q=1.2$ (dotted curves), and $q=1.3$ (solid curves), the inset showing the enlarged plot for $k_BT/W \leq 0.1$.

2. Debye model for phonons

We adopt the Debye model whose phonon density of states is given by

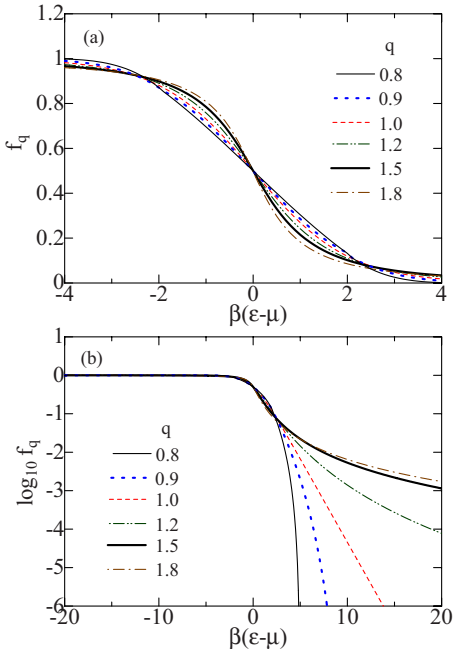

FIG. 2. (Color online) The ϵ dependence of the q-FDD of $f_q(\epsilon)$ for $q=0.8$ (solid curves), $q=0.9$ (dotted curves), $q=1.0$ (dashed curves), $q=1.2$ (double-chain curves), $q=1.5$ (bold solid curves), and $q=1.8$ (chain curves) with the (a) linear and (b) logarithmic ordinates; the results for $q \geq 1.0$ and $q<1.0$ being calculated by the EA and IA, respectively ($k_BT/W=0.1$).

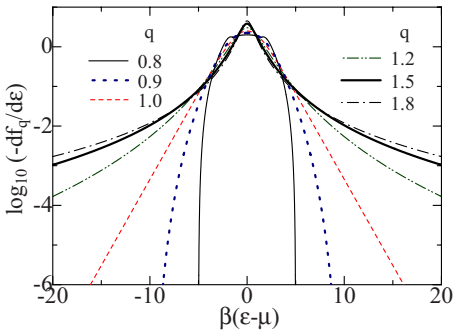

FIG. 3. (Color online) The ϵ dependence of the derivative of q-FDD, $-\partial f_q(\epsilon)/\partial\epsilon$, for $q=0.8$ (the solid curve), $q=0.9$ (the dotted curve), $q=1.0$ (the dashed curve), $q=1.2$ (the double-chain curve), $q=1.5$ (the bold solid curve), and $q=1.8$ (the chain curve) with the logarithmic ordinate; the results for $q \geq 1.0$ and $q < 1.0$ being calculated by the EA and IA, respectively ($k_B T/W=0.1$).

$$\rho(\omega) = A\omega^2 \quad \text{for } 0 < \omega \leq \omega_D, \tag{74}$$

where $A=9N_a/w_D^3$, N_a denotes the number of atoms, ω is the phonon frequency, and ω_D is the Debye cutoff frequency. By using Eq. (74) to Eqs. (9)–(12), we may obtain (with $\omega_D=1.0$ and $\mu=0$),

$$\Xi_1(u) = e^{-u\Omega_1(u)},$$

$$\Omega_1(u) = \frac{A}{180u}\left[\frac{4\pi^4}{u^3} + 15u - 60\ln(1-e^u) + 60\ln(1-\cosh u + \sinh u)\right] - \frac{A}{u^4}[u^2 Li_2(e^u) - 2uLi_3(e^u) + 2Li_4(e^u)],$$

$$N_1(u) = -\frac{A}{3u^3}[u^3 - 3u^2\ln(1-e^u) - 6uLi_2(e^u) + 6Li_3(e^u) - 6\zeta(3)],$$

$$E_1(u) = A\left[\frac{\ln(1-e^u)}{u} + \frac{3Li_2(e^u)}{u^2} - \frac{6Li_3(e^u)}{u^3} + \frac{6Li_4(e^u)}{u^4} - \frac{1}{4} - \frac{\pi^4}{15u^4}\right].$$

We have performed numerical calculations with the Debye model for $q \geq 1.0$. The temperature dependence of self-consistently calculated E_q is shown in Fig. 4 where inset shows the enlarged plots for low temperatures ($T/T_D < 0.5$). We note that E_q at low temperatures is larger for larger q.

The calculated q-BEDs $f_q(\epsilon)$ for various q values for $T/T_D=0.01$ are shown in Fig. 5 whose ordinate is in the logarithmic scale: they are indistinguishable in the linear scale. It is shown that with more increasing q, $f_q(\epsilon)$ at $\epsilon \gg \mu$ has a longer tail. Dotted and solid curves for $q < 1.0$ will be discussed in Sec. III C.

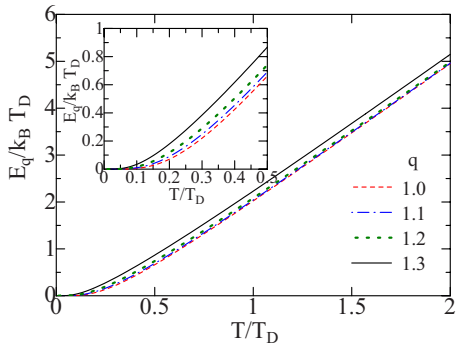

FIG. 4. (Color online) The temperature dependence of E_q of the Debye phonon model for $q=1.0$ (dashed curves), $q=1.1$ (chain curves), $q=1.2$ (dotted curves), and $q=1.3$ (solid curves); the inset showing the enlarged plot for $T/T_D \leq 0.5$.

III. INTERPOLATION APPROXIMATION

A. Analytic expressions of the generalized distributions

In Sec. II, we have discussed the generalized distributions based on the exact representation given by Eqs. (61) and (62). It is, however, difficult to calculate them because they need self-consistent calculations of N_q and E_q. If we assume

$$\left(\frac{1}{X_q}\right)e^{u(E_q-\mu N_q)}\Xi_1(u) = 1 \tag{75}$$

in Eqs. (61) and (62), we obtain the approximate generalized distributions given by

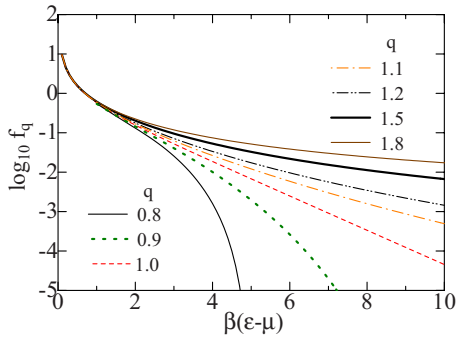

FIG. 5. (Color online) The ϵ dependence of the q-BED of $f_q(\epsilon)$ for $q=0.8$ (the solid curve), $q=0.9$ (the dotted curve), $q=1.0$ (the dashed curve), $q=1.1$ (the chain curve), $q=1.2$ (the double-chain curve), $q=1.5$ (the bold solid curves), and $q=1.8$ (the thin solid curve) with the logarithmic ordinate, the results for $q \geq 1.0$ and $q < 1.0$ being calculated by the EA and IA, respectively ($T/T_D=0.01$).

$$f_q^{\mathrm{IA}}(\epsilon,\beta)=\begin{cases}\displaystyle\int_0^\infty G\left(u;\frac{q}{q-1},\frac{1}{(q-1)\beta}\right)f_1(\epsilon,u)du & \text{for } q>1.0, \quad (76)\\ \displaystyle\frac{i}{2\pi}\int_C H\left(t;\frac{q}{1-q},\frac{1}{(1-q)\beta}\right)f_1(\epsilon,-t)dt & \text{for } q<1.0, \quad (77)\end{cases}$$

where $G(u;a,b)$ and $H(t;a,b)$ are given by Eqs. (14) and (31), respectively. Equations (76) and (77) are referred to as the *interpolation approximation* (IA) in this paper because they have the important interpolating character, as will be shown shortly (Sec. III B). Note that calculations of $f_q^{\mathrm{IA}}(\epsilon,\beta)$ by Eqs. (76) and (77) do not require N_q and E_q. Equation (76) may be regarded as a kind of the SA.

One of advantages of the IA is that we can obtain the simple analytic expressions for the q-BED and q-FDD as follows.

(1) *q-BED.* We first expand the Bose-Einstein distribution $f_1(\epsilon,\beta)$ as

$$f_1(\epsilon,\beta)=\sum_{n=0}^{\infty}e^{-(n+1)x} \quad \text{for } x>0, \quad (78)$$

where $x=\beta(\epsilon-\mu)$. Substituting Eq. (78) to Eqs. (76) and (77) and employing Eq. (5) and (27), we obtain the q-BED in the IA given by

$$f_q^{\mathrm{IA}}(\epsilon,\beta)=\sum_{n=0}^{\infty}[e_q^{-(n+1)x}]^q \quad \text{for } 0<q<3, \quad (79)$$

$$f_q^{\mathrm{IA}}(\epsilon,\beta)=\left[\frac{1}{(q-1)x}\right]^{q/(q-1)}\zeta\left(\frac{q}{q-1},\frac{1}{(q-1)x}+1\right) \quad \text{for } 1<q<3, \quad (80)$$

where $\zeta(z,a)$ denotes the Hurwitz zeta function:

$$\zeta(z,a)=\sum_{k=0}^{\infty}\frac{1}{(k+a)^z}=\frac{1}{\Gamma(z)}\int_0^\infty\frac{t^{z-1}e^{-at}}{1-e^{-t}}dt \quad \text{for Re } z>1.$$

Its derivative is given by

$$\frac{\partial f_q^{\mathrm{IA}}}{\partial x}=-\sum_{n=0}^{\infty}q(n+1)[e_q^{-(n+1)x}]^{(2q-1)} \quad \text{for } 0<q<3. \quad (81)$$

We may easily realize that $f_q(\epsilon,\beta)$ in Eq. (79) reduces to $f_1(\epsilon,\beta)$ in the limit of $q\to 1.0$ where $e_q^x\to e^x$.

(2) *q-FDD.* The Fermi-Dirac distribution $f_1(\epsilon,\beta)$ may be expanded as

$$f_1(\epsilon,\beta)=\begin{cases}\displaystyle\sum_{n=0}^{\infty}(-1)^n e^{-(n+1)x} & \text{for } x>0, \quad (82)\\ \frac{1}{2} & \text{for } x=0, \quad (83)\\ \displaystyle\sum_{n=0}^{\infty}(-1)^n e^{-n|x|} & \text{for } x<0, \quad (84)\end{cases}$$

where $x=\beta(\epsilon-\mu)$. Substituting Eqs. (82)–(84) to Eqs. (76) and (77) and employing Eq. (5) and (27), we obtain the q-FDD in the IA given by

$$f_q^{\mathrm{IA}}(\epsilon,\beta)=\begin{cases}F_q(x) & \text{for } x>0, \quad (85)\\ \frac{1}{2} & \text{for } x=0, \quad (86)\\ 1-F_q(|x|) & \text{for } x<0, \quad (87)\end{cases}$$

with

$$F_q(x)=\sum_{n=0}^{\infty}(-1)^n[e_q^{-(n+1)x}]^q \quad \text{for } 0<q<3, \quad (88)$$

$$F_q(x)=\left[\frac{1}{2(q-1)x}\right]^{q/(q-1)}\left\{\zeta\left(\frac{q}{q-1},\frac{1}{2(q-1)x}+\frac{1}{2}\right)-\zeta\left(\frac{q}{q-1},\frac{1}{2(q-1)x}+1\right)\right\} \quad \text{for } 1<q<3. \quad (89)$$

Its derivative is given by

$$\frac{\partial f_q^{\mathrm{IA}}}{\partial x}=-\sum_{n=0}^{\infty}(-1)^n q(n+1)[e_q^{-(n+1)|x|}]^{(2q-1)} \quad \text{for } 0<q<3, \quad (90)$$

which is symmetric with respect to $x=0$. The q-FDD given by Eqs. (85)–(88) reduces to $f_1(\epsilon,\beta)$ in the limit of $q\to 1.0$.

We may obtain a useful expression of the q-FDD for $|x|<1$ given by (see Appendix B 1)

$$f_q^{\mathrm{IA}}\simeq\frac{1}{2}-\frac{q}{4}x+\frac{q(2q-1)(3q-2)}{48}x^3+\cdots, \quad (91)$$

$$\frac{\partial f_q^{\mathrm{IA}}}{\partial x}\simeq-\frac{q}{4}+\frac{q(2q-1)(3q-2)}{16}x^2+\cdots \quad \text{for } 0<q<3. \quad (92)$$

In the case of $q<1.0$, summations over n in the q-BED and q-FDD [Eqs. (79) and (88)] are terminated when the condition $n+1>1/(1-q)x$ is satisfied because of the cutoff prop-

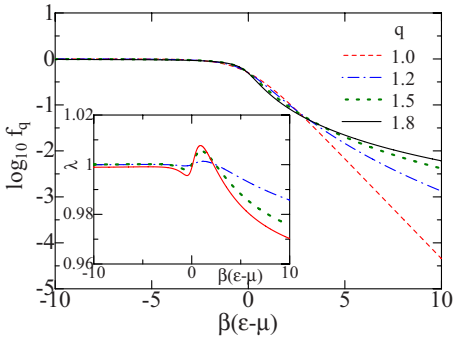

FIG. 6. (Color online) The ϵ dependence of the q-FDD of $f_q(\epsilon)$ calculated by the EA for $q=1.0$ (dashed curves), $q=1.2$ (chain curves), $q=1.5$ (dotted curves), and $q=1.8$ (solid curves) with the logarithmic ordinate; the inset showing the ratio of $\lambda=f_q^{\mathrm{IA}}(\epsilon)/f_q^{\mathrm{EA}}(\epsilon)$ $(k_BT/W=1.0)$.

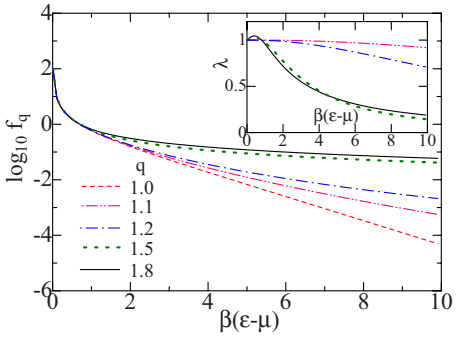

FIG. 7. (Color online) The ϵ dependence of the q-BED of $f_q(\epsilon)$ calculated by the EA for $q=1.0$ (dashed curves), $q=1.1$ (double-chain curves) $q=1.2$ (chain curves), $q=1.5$ (dotted curves), and $q=1.8$ (solid curves) with the logarithmic ordinate; the inset showing the ratio of $\lambda=f_q^{\mathrm{IA}}(\epsilon)/f_q^{\mathrm{EA}}(\epsilon)$ $(k_BT/W=0.1)$.

erties of the q-exponential function given by Eq. (70). Then the q-FDD for $q<1.0$ has the cutoff properties given by

$$f_q^{\mathrm{IA}}(\epsilon)=\begin{cases}0.0 & \text{for } \epsilon-\mu>1/(1-q)\beta, \quad (93)\\ 1.0 & \text{for } \epsilon-\mu<-1/(1-q)\beta, \quad (94)\end{cases}$$

while the q-BED has the cutoff properties given by Eq. (93). These are the same as the q-exponential distribution $p_q(\epsilon)$ given by Eq. (72).

B. Comparison with the exact approach

From Eqs. (48) and (49) with $Y_1(u)=1.0$, the q-BED and q-FDD for $q\simeq 1.0$ in the IA become

$$f_q^{\mathrm{IA}}(\epsilon,\beta)=f_1(\epsilon,\beta)+(q-1)\left[(\epsilon-\mu)\frac{\partial f_1}{\partial\epsilon}+\frac{1}{2}(\epsilon-\mu)^2\frac{\partial^2 f_1}{\partial\epsilon^2}\right]+\cdots, \quad (95)$$

which is in agreement with those in the EA given by Eq. (65) within $O(q-1)$. In the zero-temperature limit, the q-FDD reduces to

$$f_q^{\mathrm{IA}}(\epsilon,T=0)=\Theta(\mu-\epsilon). \quad (96)$$

In the opposite high-temperature limit, the q-BED and q-FDD become

$$f_q^{\mathrm{IA}}(\epsilon,\beta\to 0)\propto[e_q^{-x}]^q. \quad (97)$$

Equations (96) and (97) agree with Eqs. (67) and (68), respectively, for the EA. Thus the generalized distributions in the IA have the interpolation properties, yielding results in agreement with those in the EA within $O(q-1)$ and in high- and low-temperature limits.

C. Numerical calculations

Numerical calculations of $f_q^{\mathrm{IA}}(\epsilon,\beta)$ $[\equiv f_q^{\mathrm{IA}}(\epsilon)]$ have been performed. Results of the FDD of $f_q^{\mathrm{EA}}(\epsilon)$ in the EA for $q>1.0$ and $k_BT/W=1.0$ are shown in Fig. 6. With more increasing q, the distributions have longer tails, as shown in Fig. 2 for $k_BT/W=0.1$. The result in the IA is in good agreement with the EA because the ratio defined by $\lambda\equiv f_q^{\mathrm{IA}}(\epsilon)/f_q^{\mathrm{EA}}(\epsilon)$ is $0.97\lesssim\lambda\lesssim 1.01$ for $-10<\epsilon<10$ as shown in the inset. The ϵ dependence of the BED of $f_q^{\mathrm{EA}}(\epsilon)$ in the EA for $q>1.0$ and $T/T_D=0.1$ is plotted in Fig. 7 which shows similar behavior to those for $T/T_D=0.01$ shown in Fig. 6. Its inset shows that the ratio of λ is $0.7\lesssim\lambda\lesssim 1.0$ for $1.0<q\lesssim 1.2$. These calculations justify, to some extent, the distribution in the IA given by Eqs. (80), (85)–(87), and (89).

We have calculated the q-BED and q-FDD also for $q<1.0$ by using Eqs. (79) and (85)–(88). Dotted and solid curves in Fig. 2 show the q-FDD of $f_q^{\mathrm{IA}}(\epsilon)$ for $q=0.9$ and $q=0.8$, respectively. Their derivatives of $-\partial f_q^{\mathrm{IA}}(\epsilon)/\partial\epsilon$ for $q=0.9$ and $q=0.8$ are plotted by the dotted and solid curves, respectively, in Fig. 3. Dotted and solid curves in Fig. 5 show

TABLE I. Generalized distributions in the limits of $q\to 1$, $T\to 0$, and $\beta\to 0$. $f_1=1/(e^{\beta(\epsilon-\mu)}\mp 1)$: $\Theta(x)$—the Heaviside function; e_q^x, q-exponential function.

Method	$q\to 1$	$T\to 0$ (FDD)	$\beta\to 0$
EA[a]	$f_1+(q-1)[(\epsilon-\mu)\frac{\partial f_1}{\partial\epsilon}+\frac{1}{2}(\epsilon-\mu)^2\frac{\partial^2 f_1}{\partial\epsilon^2}]+\cdots$	$\Theta(\mu-\epsilon)$	$[e_q^{-\beta(\epsilon-\mu)}]^q$
IA[b]	$f_1+(q-1)[(\epsilon-\mu)\frac{\partial f_1}{\partial\epsilon}+\frac{1}{2}(\epsilon-\mu)^2\frac{\partial^2 f_1}{\partial\epsilon^2}]+\cdots$	$\Theta(\mu-\epsilon)$	$[e_q^{-\beta(\epsilon-\mu)}]^q$
FA[c]	$f_1-\frac{1}{2}(q-1)\beta(\epsilon-\mu)^2\frac{\partial f_1}{\partial\epsilon}+\cdots$	$\Theta(\mu-\epsilon)$	$e_q^{-\beta(\epsilon-\mu)}$
SA[d]	$f_1+\frac{1}{2}(q-1)(\epsilon-\mu)^2\frac{\partial^2 f_1}{\partial\epsilon^2}+\cdots$	$\Theta(\mu-\epsilon)$	$e_q^{-\beta(\epsilon-\mu)}$

[a]The exact approach (the present study).
[b]The interpolation approximation (the present study).
[c]The factorization approximation [24].
[d]The superstatiscal approximation [49].

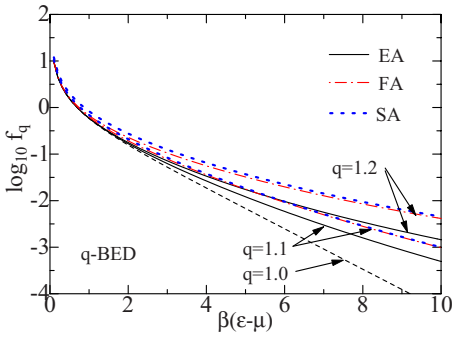

FIG. 8. (Color online) The ϵ dependence of the q-BED of $f_q(\epsilon)$ for $q=1.1$ and 1.2 calculated by the EA (solid curves), FA (chain curves), and SA (dotted curves) with the logarithmic ordinate, $f_1(\epsilon)$, for $q=1.0$ being plotted by the dashed curve for a comparison $(T/T_D=0.01)$.

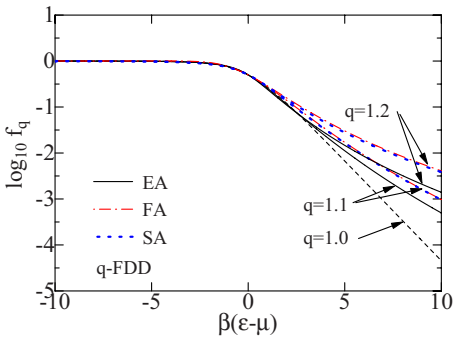

FIG. 9. (Color online) The ϵ dependence of the q-FDD of $f_q(\epsilon)$ for $q=1.1$ and 1.2 calculated by the EA (the solid curve), FA (the chain curve), and SA (the dotted curve) with the logarithmic ordinate, $f_1(\epsilon)$ for $q=1.0$ being plotted by the dashed curve for a comparison $(k_BT/W=0.1)$.

the q-BED of $f_q^{\mathrm{IA}}(\epsilon)$ for $q=0.9$ and $q=0.8$, respectively. With more decreasing q from unity, the curvatures of $f_q(\epsilon)$ in both q-BED and q-FDD become more significant. The cutoff properties in the q-FDD and q-BED given by Eqs. (93) and (94) are realized in Figs. 2 and 5. We expect that $f_q^{\mathrm{IA}}(\epsilon)$ in the case of $q<1.0$ is a good approximation of the q-BED and q-FDD as in the case of $q>1.0$.

IV. DISCUSSION

A. Comparison with previous studies

It is interesting to compare our results to those previously obtained with some approximations.

(A) *Factorization approximation.* Büyükkilic *et al.* [24] derived the q-BED and q-FDD given by

$$f_q^{\mathrm{FA}}(\epsilon,\beta)=\frac{1}{\{e_q[-\beta(\epsilon-\mu)]\}^{-1}\mp 1}, \tag{98}$$

adopting the FA given by

$$Q=\left[1-(1-q)\sum_{n=1}^{N}x_n\right]^{1/(1-q)} \tag{99}$$

$$\simeq\prod_{n=1}^{N}[1-(1-q)x_n]^{1/(1-q)} \tag{100}$$

to evaluate the grand-canonical partition function, the upper (lower) sign in Eq. (98) being applied to boson (fermion).

It is noted that if we assume the factorization approximation, $[e_q^{-(n+1)x}]^q\simeq(e_q^{-x})^q[(e_q^{-x})^q]^n$ in $f_q^{\mathrm{IA}}(\epsilon)$ [Eqs. (79) and (88)], we obtain

$$f_q(\epsilon,\beta)\simeq\frac{1}{\{e_q[-\beta(\epsilon-\mu)]\}^{-q}\mp 1}, \tag{101}$$

which is similar to Eq. (98) [41,55].

(B) *The superstatistical approximation.* In the SA, the generalized distribution is expressed as a superposition of $f_1(\epsilon)$ [8,9],

$$f_q^{\mathrm{SA}}(\epsilon,\beta)=\int_0^\infty G\left(u;\frac{1}{q-1},\frac{1}{(q-1)\beta}\right)f_1(\epsilon,u)du, \tag{102}$$

which is similar to but different from $f_q^{\mathrm{IA}}(\epsilon,\beta)$ given by Eq. (76). Recently the q-FDD equivalent to Eq. (98) is obtained by employing the SA in a different way [49].

The properties of the generalized distributions of the EA, IA, FA, and SA in the limits of $q\to 1.0$, $T=0$, and $\beta\to 0.0$ are compared in Table I. The result of the IA agrees with that of the EA within $O(q-1)$ as mentioned before. However, the $O(q-1)$ contributions in the FA and SA are different from

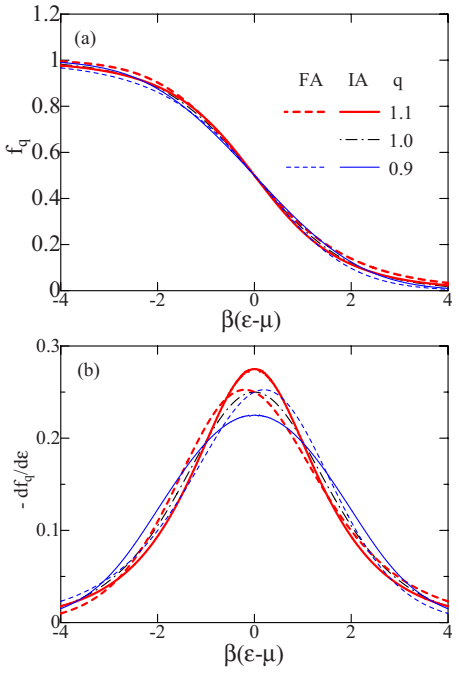

FIG. 10. (Color online) The ϵ dependences of (a) the q-FDDs of $f_q(\epsilon)$ and (b) its derivative of $-\partial f_q(\epsilon)/\partial\epsilon$ calculated by the IA for $q=0.9$ (solid curves) and 1.1 (bold solid curves) and those calculated by the FA for $q=0.9$ (dashed curves) and 1.1 (bold dashed curves); results for $q=1.0$ being plotted by chain curves for a comparison.

that in the EA. In the zero-temperature limit, all the q-FDDs reduce to $\Theta(\mu-\epsilon)$. In the opposite high-temperature limit, the generalized distributions in the FA and SA reduce to $e_q^{-\beta\epsilon}$, while those in the EA and IA become $[e_q^{-\beta\epsilon}]^q$, where the power index q arises from the escort probability in the OLM-MEM given by Eq. (71) [5,6].

Figure 8 shows q-BED for $q=1.1$ and $q=1.2$ calculated by the FA, SA, and EA with the logarithmic ordinate. For a comparison, we show $f_q(\epsilon)$ for $q=1.0$ by dashed curves. The difference among $f_q(\epsilon)$'s of the three methods is clearly realized: tails in the q-BED of the FA and SA are overestimated.

Figure 9 shows q-FDD for $q=1.1$ and $q=1.2$ calculated by the EA, FA, and SA with the logarithmic ordinate (for more detailed $f_q^{\mathrm{FA}}(\epsilon)$, see Fig. 1 of Ref. [49]). Tails in the FA and SA are larger than that in the EA, as in the case of the q-BED shown in Fig. 8.

Figures 10(a) and 10(b) show the q-FDD and its derivative, respectively, calculated in the IA and FA. For $q=0.9$, $f_q^{\mathrm{FA}}(\epsilon)$ at $\epsilon<\mu$ is much reduced than $f_q^{\mathrm{IA}}(\epsilon)$. For $q=1.1$, on the contrary, $f_q^{\mathrm{FA}}(\epsilon)$ at $\epsilon>\mu$ is much increased than $f_q^{\mathrm{IA}}(\epsilon)$. These lead to an overestimate of electron excitations across the Fermi level μ in the FA. Furthermore $-\partial f_q^{\mathrm{FA}}(\epsilon)/\partial\epsilon$ in the FA is not symmetric with respect to $\epsilon=\mu$ in contrast to that in the IA.

The FA was criticized in Refs. [25,26] but justified in Ref. [27]. The dismissive study [25] was based on a simulation with $N=2$. In contrast, the affirmative study [27] performed simulations with $N=10^5$ and 10^{15}. Lenzi *et al.* [26] criticized the FA, applying the EA [50,51] to independent harmonic oscillators with $N\leq 100$. Our results are consistent with Refs. [25,26]. The FA given by Eq. (100) has been explicitly or implicitly employed in many studies not only for quantum but also for classical nonextensive systems. It would be necessary to examine the validity of these studies using the FA from the viewpoint of the exact representation [50,51,60,61].

By using Eqs. (5) and (27), we may rewrite Q in Eq. (99) as

$$Q=[1-(1-q)x_1]^{1/(1-q)}\otimes_q\cdots\otimes_q[1-(1-q)x_N]^{1/(1-q)}, \tag{103}$$

$$Q=\begin{cases}\displaystyle\int_0^\infty G\left(u;\frac{1}{q-1},\frac{1}{q-1}\right)\prod_{n=1}^N e^{-ux_n}du & \text{for } q>1.0, \quad (104)\\ \displaystyle\frac{i}{2\pi}\int_C H\left(t;\frac{1}{1-q},\frac{1}{1-q}\right)\prod_{n=1}^N e^{tx_n}dt & \text{for } q<1.0, \quad (105)\end{cases}$$

where $\otimes_q$ denotes the q product defined by [62]

$$x\otimes_q y\equiv[x^{1-q}+y^{1-q}-1]^{1/(1-q)}. \tag{106}$$

Equations (104) and (105) are the integral representations of the q product given by Eq. (103). The result of the FA in Eq. (100) is derived if we may exchange the order of integral and product in Eqs. (104) and (105), which is of course forbidden.

B. Generalized Sommerfeld expansion

We will investigate the generalized Sommerfeld expansion for an arbitrary function $\phi(\epsilon)$ with the q-FDD of $f_q(\epsilon)$ given by [49]

$$I=\int\phi(\epsilon)f_q(\epsilon)d\epsilon \tag{107}$$

$$=\int^\mu\phi(\epsilon)d\epsilon+\sum_{n=1}^\infty c_{n,q}(k_BT)^n\phi^{(n-1)}(\mu), \tag{108}$$

with

$$c_{n,q}=-\frac{\beta^n}{n!}\int(\epsilon-\mu)^n\frac{\partial f_q(\epsilon)}{\partial\epsilon}d\epsilon. \tag{109}$$

Substituting $f_q(\epsilon)$ in the EA given by Eq. (65) to Eq. (109) and using integrals by part, we obtain $c_{n,q}$ for even n,

$$\frac{c_{n,q}^{\mathrm{EA}}}{c_{n,1}}=\begin{cases}1+\dfrac{n(n-1)}{2}(q-1)+\cdots & \text{for even } n, \quad (110)\\ 1+(q-1)+\cdots & \text{for } n=2, \quad (111)\\ 1+6(q-1)+\cdots & \text{for } n=4, \quad (112)\end{cases}$$

while $c_{n,q}=0$ for odd n, where $c_{n,1}$ denotes the relevant expansion coefficient for $q=1.0$: $c_{2,1}=\pi^2/6(=1.645)$ and $c_{4,1}=7\pi^4/360(=1.894)$. Equation (110) shows that $c_{n,q}$ is increased with increasing q.

TABLE II. $O(q-1)$ contributions to $c_{n,q}$ $(n=1-4)$ of the generalized Sommerfeld expansion coefficients.

Method	$c_{1,q}$	$c_{2,q}$	$c_{3,q}$	$c_{4,q}$
EA[a]	0	$\frac{\pi^2}{6}[1+(q-1)]$	0	$\frac{7\pi^4}{360}[1+6(q-1)]$
IA[b]	0	$\frac{\pi^2}{6}[1+(q-1)]$	0	$\frac{7\pi^4}{360}[1+6(q-1)]$
FA[c]	$\frac{\pi^2}{6}(q-1)$	$\frac{\pi^2}{6}\{1+O[(q-1)^2]\}$	$\frac{7\pi^4}{60}(q-1)$	$\frac{7\pi^7}{360}\{1+O[(q-1)^2]\}$
SA[d]	0	$\frac{\pi^2}{6}[1+3(q-1)]$	0	$\frac{7\pi^4}{360}[1+10(q-1)]$

[a]The exact approach (the present study).
[b]The interpolation approximation (the present study).
[c]The factorization approximation [24].
[d]The superstatiscal approximation [49].

By using $f_q^{\mathrm{IA}}(\epsilon)$ in the IA, we may obtain $c_{n,q}$ given by (for details, see Appendix B 2)

$$\frac{c_{n,q}^{\mathrm{IA}}}{c_{n,1}} = \begin{cases} \dfrac{\Gamma\left(\dfrac{1}{q-1}+1-n\right)}{(q-1)^n\Gamma\left(\dfrac{1}{q-1}+1\right)} & \text{for even } n,q>1 \quad (113) \\ \dfrac{\Gamma\left(\dfrac{q}{1-q}+1\right)}{(1-q)^n\Gamma\left(\dfrac{q}{1-q}+1+n\right)} & \text{for even } n,q<1, \quad (114) \\ \dfrac{1}{2-q} & \text{for } n=2, \quad (115) \\ \dfrac{1}{(2-q)(3-2q)(4-3q)} & \text{for } n=4. \quad (116) \end{cases}$$

It is easy to see that Eqs. (115) and (116) are in agreement with Eq. (111) and (112), respectively, of the EA within $O(q-1)$.

A simple calculation using $f_q^{\mathrm{SA}}(\epsilon)$ leads to

$$\frac{c_{n,q}^{\mathrm{SA}}}{c_{n,1}} = \begin{cases} \dfrac{\Gamma\left(\dfrac{1}{q-1}-n\right)}{(q-1)^n\Gamma\left(\dfrac{1}{q-1}\right)} & \text{for even } n,q>1 \\ \dfrac{1}{(2-q)(3-2q)} & \text{for } n=2 \\ \dfrac{1}{(2-q)(3-2q)(4-3q)(5-4q)} & \text{for } n=4, \end{cases} \quad (117)$$

which are similar to but different from those given by Eqs. (115) and (116).

The Sommerfeld expansion coefficients in the FA may be calculated with the use of $f_q^{\mathrm{FA}}(\epsilon)$ [49]. A comparison among the $O(q-1)$ contributions to $c_{n,q}$ $(n=1-4)$ in the four methods of EA, IA, FA, and SA is made in Table II. The results of the IA coincide with those of the EA. The $O(q-1)$ contributions to $c_{2,q}$ and $c_{4,q}$ in the SA are three and 5/3 times larger, respectively, than those in the EA. The $O(q-1)$ contributions to $c_{2,q}$ and $c_{4,q}$ in the FA are vanishing. It is noted that $c_{1,q}^{\mathrm{FA}} \neq 0$ and $c_{3,q}^{\mathrm{FA}} \neq 0$ in contrast with the results of $c_{1,q}=c_{3,q}=0$ in the EA, IA, and SA. This is due to a lack of the symmetry in $-\partial f_q^{\mathrm{FA}}(\epsilon)/\partial\epsilon$ with respect to $\epsilon=\mu$ as shown in Fig. 10(b).

Figure 11(a) shows the q dependence of coefficients of $c_{n,q}/c_{n,1}$ for $n=2$ and 4 calculated by the four methods. Circles and squares express $c_{n,q}^{\mathrm{EA}}$ for $n=2$ and 4, respectively, calculated by the EA for $k_BT/W=0.1$ (Fig. 1). Solid curves express $c_{n,q}^{\mathrm{IA}}$ in the IA. The coefficient for $n=2$ $(n=4)$ in the IA is in good agreement with the result in the EA for $1.0 \lesssim q \lesssim 1.5$ $(1.0 \lesssim q \lesssim 1.2)$. $c_{n,q}^{\mathrm{SA}}$ shown by chain curves are overestimated compared to $c_{n,q}^{\mathrm{EA}}$ and $c_{n,q}^{\mathrm{IA}}$. Dashed curves denoting $c_{n,q}^{\mathrm{FA}}$ [49] are plotted only for $0.8 \lesssim q \lesssim 1.2$ because the FA is considered to be valid for a small $|q-1|$ [23]. The q dependence of $c_{n,q}^{\mathrm{FA}}$ is qualitatively different from

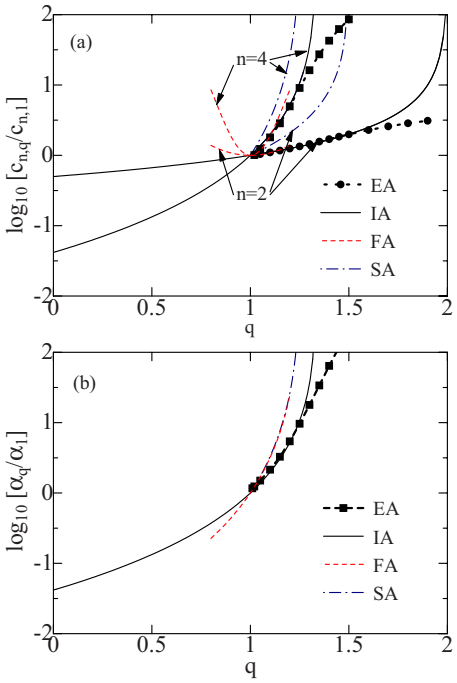

FIG. 11. (Color online) (a) The q dependence of $c_{n,q}/c_{n,1}$ for $n=2$ and 4 of the generalized Sommerfeld expansion coefficients [Eq. (108)] with the q-FDD and (b) the q dependence of α_q/α_1 of the coefficients in the low-temperature phonon specific heat with the q-BED, calculated by the EA (circles and squares), IA (solid curves), FA (dashed curves) [49], and SA (chain curves): the result of the SA is indistinguishable from that of the FA in (b) (see text).

those of the EA, IA, and SA: $c_{n,q}^{\mathrm{FA}}$ is symmetric with respect to $q=1.0$ whereas those in other three methods are monotonously increased with increasing q.

The energy of electron systems at low temperatures may be calculated with the use of the generalized Sommerfeld expansion. By using Eqs. (108) and (110) for Eq. (73) with $\phi(\epsilon)=\epsilon\rho(\epsilon)$, we obtain the energy given by

$$E_q(T) \simeq E_q(0) + c_{2,q}(k_B T)^2 \rho(\mu) + \cdots, \tag{118}$$

from which the low-temperature electronic specific heat is given by

$$C_q(T) \simeq \gamma_q T + \cdots, \tag{119}$$

with

$$\frac{\gamma_q}{\gamma_1} = \frac{c_{2,q}}{c_{2,1}}, \tag{120}$$

$$\gamma_1 = \frac{\pi^2}{3} k_B^2 \rho(\mu), \tag{121}$$

where γ_1 is the linear-T expansion coefficient for $q=1.0$.

The inset of Fig. 1 shows that the calculated energy E_q at low temperatures in the electron model is larger for a larger q, which is consistent with larger γ_q and $c_{2,q}$ for a larger q as shown in Fig. 11(a).

C. Low-temperature phonon specific heat

We consider the phonon specific heat at low temperatures. By using Eqs. (60) and (65), we obtain

$$C_q \simeq \alpha_q T^3 + \cdots, \tag{122}$$

with

$$\frac{\alpha_q^{\mathrm{EA}}}{\alpha_1} = 1 + 6(q-1) + \cdots, \tag{123}$$

$$\alpha_1 = \left(\frac{12\pi^4}{5}\right) N_a k_B, \tag{124}$$

where α_1 is the relevant coefficient for $q=1.0$.

The coefficients of low-temperature phonon specific heat α_q in the IA, SA, and FA are given by (for details, see Appendix B 3)

$$\frac{\alpha_q^{\mathrm{IA}}}{\alpha_1} = \frac{1}{(2-q)(3-2q)(4-3q)}, \tag{125}$$

$$\frac{\alpha_q^{\mathrm{SA}}}{\alpha_1} = \frac{1}{(2-q)(3-2q)(4-3q)(5-4q)}, \tag{126}$$

$$\frac{\alpha_q^{\mathrm{FA}}}{\alpha_1} = 1 + O[(q-1)^2], \tag{127}$$

where the $O(q-1)$ contribution to α_q^{FA} is vanishing [49]. Equation (125) shows that α_q^{IA} agrees with α_q^{EA} within $O(q-1)$ and that the α_q^{IA} is related with $c_{4,q}^{\mathrm{IA}}$ as $\alpha_q^{\mathrm{IA}}/\alpha_1 = c_{4,q}^{\mathrm{IA}}/c_{4,1}$.

Coefficients of α_q/α_1 calculated by the four methods are plotted as a function of q in Fig. 11(b). Squares denote the result of numerical calculation by the EA for $T/T_D=0.01$ (Fig. 4). The solid curve expresses α_q^{IA}, which is in good agreement with the result of the EA for $1.0 \leq q \lesssim 1.2$ but deviates from it at $q \gtrsim 1.2$. Dashed and chain curves show α_q calculated by the FA and SA, respectively. It is interesting that the result of the SA nearly coincides with that of the FA for $1.0 \leq q \lesssim 1.2$, where both the results of the SA and FA are overestimated compared to the EA. The inset of Fig. 4 shows that the energy E_q at low temperatures in the Debye model is larger for larger q, which is consistent with the q dependence of α_q shown in Fig. 11(b).

V. CONCLUDING REMARKS

It is well known that in nonextensive classical statistics, the nonextensivity arises from the long-range interaction, the long-time memory, and a multifractal-like space time [2]. The metastable state or quasistationary state is characterized by long-range interaction and/or fluctuations of intensive quantities (e.g., the inverse temperature) [10]. For example, in the long-range-interacting gravitating systems, the physical quantities are not extensive: the velocity distribution obeys the power law and the stable equilibrium state is lacking, which lead to negative specific heat [63]. The situation is the same also in nonextensive quantum statistics. It has been

reported that the observed black-body radiation may be explained by the nonextensivity of the order of $|q-1| \sim 10^{-4}-10^{-5}$, which is attributed to the long-range Coulomb interaction [21]. Memory effect and long-range interaction cannot be neglected in weakly nonideal plasma of stellar core [64]. In addition to the large systems where the interactions may be truly long range, one should consider small systems where the range of the interactions is of the order of the system size. Small-size systems would not be extensive, and many similarities with the long-range case will be realized. Indeed, the negative specific heat is observed in 147 sodium clusters [65]. Magnetic properties in nanomagnets may be different from those in large-size ones [66]. Small drops of quantum fluids may undergo a Bose-Einstein condensation. Thanks to recent development in the evaporation cooling technique, it becomes possible to study Bose-Einstein condensation in an extremely diluted fluid where the long-range interactions play essential roles in the condensate stability. Artificial sonic or optical black hole [67,68] represents an intrigue quantum catastrophic phenomenon. Only little is known about the thermodynamics of these quantum systems. Experimental and theoretical studies on these subjects deepen our understanding of basic quantum phenomena.

To summarize, we have discussed the generalized distributions of q-BED and q-FDD in nonextensive quantum statistics based on the EA [50,51] and IA. Results obtained are summarized as follows:

(i) with increasing q above $q=1.0$, the q-BED and q-FDD have long tails, while they have compact distributions with decreasing q from unity,

(ii) the coefficients in the generalized Sommerfeld expansion, the linear-T coefficient of electronic specific heat, and the T^3 coefficient of phonon specific heat are increased with increasing q above unity, whereas they are decreased with decreasing q below unity,

(iii) the $O(q-1)$ contributions in the EA agree with those in the AA based on the OLM-MEM [5] as well as the un-normalized MEM [3], and

(iv) the generalized distributions given by simple expressions in the IA proposed in this study yield results in agreement with those obtained by the EA within $O(q-1)$ and high- and low-temperature limits.

As for item (iv), the q-BED and q-FDD in the IA are expected to be useful and to play important roles in the nonextensive quantum statistics [61].

ACKNOWLEDGMENT

This work was partly supported by a Grant-in-Aid for Scientific Research from the Japanese Ministry of Education, Culture, Sports, Science and Technology.

APPENDIX A: THE $(q-1)$ EXPANSION IN THE UN-NORMALIZED MEM

Tsallis *et al.* [21] developed the AA to investigate the nonextensivity in the observed black-body radiation by using the un-normalized MEM [3]. We will show that the EA with the un-normalized MEM yields the result in agreement with the AA within $O(q-1)$. Calculations of the q-BED and q-FDD for $q \simeq 1.0$ are presented.

1. Un-normalized MEM

An application of the un-normalized MEM to the Hamiltonian $\hat{H}$ yields the optimized density matrix given by [3]

$$\hat{\rho}_q = \frac{1}{Z_q}[1-(1-q)\beta\hat{H}]^{1/(1-q)}, \tag{A1}$$

$$Z_q(\beta) = \mathrm{Tr}\{[1-(1-q)\beta\hat{H}]^{1/(1-q)}\}. \tag{A2}$$

The expectation value of the operator $\hat{O}$ is given by

$$O_q(\beta) \equiv \langle \hat{O} \rangle_q = \mathrm{Tr}\{\hat{\rho}_q^q \hat{O}\} \tag{A3}$$

$$= \frac{1}{Z_q^q}\mathrm{Tr}\{[1-(1-q)\beta\hat{H}]^{q/(1-q)}\hat{O}\}. \tag{A4}$$

2. Exact approach

With the use of the exact representations given by Eqs. (5) and (27), Eqs. (A2) and (A4) are expressed by

$$Z_q = \begin{cases} \displaystyle\int_0^\infty G\left(u; \frac{1}{q-1}, \frac{1}{(q-1)\beta}\right) Z_1(u)du & \text{for } q>1, \quad \text{(A5)} \\ \displaystyle\frac{i}{2\pi}\int_C H\left(t; \frac{1}{1-q}, \frac{1}{(1-q)\beta}\right) Z_1(-t)dt & \text{for } q<1, \quad \text{(A6)} \end{cases}$$

$$O_q = \begin{cases} \displaystyle\frac{1}{Z_q^q}\int_0^\infty G\left(u; \frac{1}{q-1}+1, \frac{1}{(q-1)\beta}\right) Z_1(u)O_1(u)du & \text{for } q>1, \quad \text{(A7)} \\ \displaystyle\frac{i}{2\pi Z_q^q}\int_C H\left(t; \frac{1}{1-q}-1, \frac{1}{(1-q)\beta}\right) Z_1(-t)O_1(-t)dt & \text{for } q<1, \quad \text{(A8)} \end{cases}$$

with

$$O_1(u) = \frac{\mathrm{Tr}\{e^{-u\hat{H}}\hat{O}\}}{Z_1(u)}, \tag{A9}$$

$$Z_1(u) = \mathrm{Tr}\{e^{-u\hat{H}}\}, \tag{A10}$$

where C denotes the Hankel contour and $G(u;a,b)$ and $H(t;a,b)$ are given by Eqs. (14) and (31), respectively. In order to evaluate Eqs. (A5)–(A8), we expand their integrands around $u=\beta$ and $-t=\beta$ as is made in Sec. II C. By using Eqs. (22), (23), (35), and (36), we obtain

$$Z_q = Z_1 + \frac{1}{2}(q-1)\beta^2\frac{\partial^2 Z_1}{\partial\beta^2} + \cdots, \tag{A11}$$

$$O_q = \frac{1}{Z_q^q}\left[O_1 + (q-1)\beta\frac{\partial}{\partial\beta}(Z_1O_1) + \frac{1}{2}(q-1)\beta^2\frac{\partial^2}{\partial\beta^2}(Z_1O_1) + \cdots\right]. \tag{A12}$$

By using the relations given by

$$\frac{\partial Z_1}{\partial\beta} = -\langle\hat{H}\rangle_1 Z_1,$$

$$\frac{\partial^2 Z_1}{\partial\beta^2} = \langle\hat{H}^2\rangle_1 Z_1,$$

$$\frac{\partial O_1}{\partial\beta} = \langle H\rangle_1\langle O\rangle_1 - \langle\hat{H}\hat{O}\rangle_1,$$

$$\frac{\partial^2 O_1}{\partial\beta^2} = \langle\hat{H}^2\hat{O}\rangle_1 - \langle\hat{H}^2\rangle_1\langle\hat{O}\rangle_1 + 2[\langle\hat{H}\rangle_1^2\langle\hat{O}\rangle_1 - \langle\hat{H}\hat{O}\rangle_1\langle\hat{H}\rangle_1],$$

we finally obtain the $O(q-1)$ expansion of O_q given by

$$O_q \simeq O_1 + (1-q)\Big(O_1\ln Z_1 + \beta\langle\hat{H}\hat{O}\rangle_1 + \tfrac{1}{2}\beta^2[\langle\hat{H}^2\rangle_1 O_1 - \langle\hat{H}^2\hat{O}\rangle_1]\Big) + \cdots, \tag{A13}$$

which agrees with Eq. (7) in Ref. [21] derived by the AA.

(1) *q -BED*. In order to calculate the q-BED, we consider $\hat{O}=\hat{n}_k$ with the Hamiltonian for bosons given by

$$\hat{H} = \sum_k (\epsilon_k - \mu)\hat{n}_k, \tag{A14}$$

where $\hat{n}_k$ and ϵ_k stand for the number operator and the energy of the state k. We obtain

$$\langle\hat{n}_k\rangle_1 = \frac{1}{e^x-1} = f_1(\epsilon_k) \equiv f_1 \quad [x=\beta(\epsilon_k-\mu)], \tag{A15}$$

$$\langle\hat{n}_k\hat{H}\rangle_1 = (\epsilon_k-\mu)e^x f_1^2 + f_1E_1, \tag{A16}$$

$$\langle\hat{H}^2\rangle_1 = E_1^2 + E_2 + E_3, \tag{A17}$$

$$\langle\hat{n}_k\hat{H}^2\rangle_1 = 2(\epsilon_k-\mu)^2 f_1^3 - 2(\epsilon_k-\mu)f_1^2E_1 + f_1(E_1^2+E_2+E_3), \tag{A18}$$

with

$$E_1 = \sum_k (\epsilon_k-\mu)f_1,$$

$$E_2 = \sum_k (\epsilon_k-\mu)^2 f_1,$$

$$E_3 = \sum_k (\epsilon_k-\mu)^2 f_1^2.$$

Substituting Eqs. (A15)–(A18) to Eq. (A13), we obtain

$$f_q \simeq f_1 + (1-q)\{f_1\ln Z_1 + \beta[(\epsilon_k-\mu)e^x f_1^2 + f_1E_1]\} - \frac{(1-q)\beta^2}{2}[(\epsilon_k-\mu)^2e^x(e^x+1)f_1^3 + 2(\epsilon_k-\mu)e^x f_1^2E_1] + \cdots. \tag{A19}$$

Tsallis *et al.* [21] employed a one-component boson Hamiltonian given by

$$\hat{H} = \hbar\omega\hat{n} \equiv \epsilon\hat{n}, \tag{A20}$$

which yields

$$\langle\hat{n}_k\rangle_1 = \frac{1}{e^x-1} \equiv f_1 \quad (x=\beta\epsilon), \tag{A21}$$

$$\langle\hat{n}\hat{H}\rangle_1 = \epsilon(e^x+1)f_1, \tag{A22}$$

$$\langle\hat{H}^2\rangle_1 = \epsilon^2(e^x+1)f_1^2, \tag{A23}$$

$$\langle\hat{n}\hat{H}^2\rangle_1 = \epsilon^2(e^{2x}+4e^x+1)f_1^3. \tag{A24}$$

A substitution of Eqs. (A21)–(A24) to Eq. (A13) leads to

$$f_q \simeq f_1 + (1-q)\Big[f_1\ln Z_1 + x(e^x+1)f_1^2 - \tfrac{1}{2}x^2e^x(e^x+3)f_1^3\Big] + \cdots, \tag{A25}$$

which is different from Eq. (A19) with $\mu=0$ because of the difference in the adopted Hamiltonians given by Eqs. (A14) and (A20).

(2) *q -FDD*. We consider $\hat{O}=\hat{n}_k$ with the Hamiltonian for fermions given by

$$\hat{H} = \sum_k (\epsilon_k-\mu)\hat{n}_k, \tag{A26}$$

which leads to

$$\langle\hat{n}_k\rangle_1 = \frac{1}{e^x+1} = f_1(\epsilon_k) \equiv f_1 \quad [x=\beta(\epsilon_k-\mu)], \tag{A27}$$

$$\langle\hat{n}_k\hat{H}\rangle_1 = (\epsilon_k-\mu)f_1(1-f_1) + f_1E_1, \tag{A28}$$

$$\langle\hat{H}^2\rangle_1 = E_1^2 + E_2 - E_3, \tag{A29}$$

$$\langle \hat{n}_k \hat{H}^2 \rangle_1 = (\epsilon_k - \mu)^2 f_1(1-f_1)(1-2f_1) + 2(\epsilon_k - \mu) f_1(1-f_1)E_1 + f_1(E_1^2 + E_2 - E_3). \quad \text{(A30)}$$

Substituting Eqs. (A27)–(A30) to Eq. (A13), we obtain

$$f_q \simeq f_1 + (1-q)\{f_1 \ln Z_1 + \beta[(\epsilon_k - \mu)f_1(1-f_1) + f_1 E_1]\} - \frac{(1-q)\beta^2}{2}[(\epsilon_k - \mu)^2 f_1(1-f_1)(1-2f_1) + 2(\epsilon_k - \mu)f_1(1-f_1)E_1] + \cdots. \quad \text{(A31)}$$

When assuming a one-component fermion Hamiltonian given by

$$\hat{H} = (\epsilon_k - \mu)\hat{n}_k, \quad \text{(A32)}$$

we obtain

$$\langle \hat{n}_k \rangle_1 = \frac{1}{e^x + 1} \equiv f_1 \quad [x = \beta(\epsilon_k - \mu)], \quad \text{(A33)}$$

$$\langle \hat{n}_k \hat{H} \rangle_1 = (\epsilon_k - \mu) f_1, \quad \text{(A34)}$$

$$\langle \hat{H}^2 \rangle_1 = (\epsilon_k - \mu)^2 f_1, \quad \text{(A35)}$$

$$\langle \hat{n}_k \hat{H}^2 \rangle_1 = (\epsilon_k - \mu)^2 f_1. \quad \text{(A36)}$$

Substituting Eqs. (A33)–(A36) to Eq. (A13), we obtain

$$f_q \simeq f_1 + (1-q)\left[f_1 \ln Z_1 + \beta(\epsilon - \mu)f_1 - \tfrac{1}{2}\beta^2(\epsilon - \mu)^2 e^{\beta(\epsilon-\mu)} f_1^2\right] + \cdots. \quad \text{(A37)}$$

The difference between Eqs. (A31) and (A37) is due to the difference in the adopted Hamiltonians given by Eqs. (A26) and (A32). It is noted that the $(q-1)$ expansion of q-FDD in the FA is given by

$$f_q^{\mathrm{FA}} \simeq f_1 - \frac{(1-q)}{2}\beta^2(\epsilon - \mu)^2 e^{\beta(\epsilon-\mu)} f_1^2 + \cdots, \quad \text{(A38)}$$

whose $O(q-1)$ term corresponds to the last term of Eq. (A37) derived by the un-normalized MEM. This is due to the fact that to adopt the one-component Hamiltonian given by Eq. (A32) means to use the factorization approximation from the beginning.

Equation (A19) for q-BED and Eq. (A31) for q-FDD are expressed in a unified way as

$$f_q \simeq f_1 + (1-q)\left[f_1 \ln Z_1 + \beta E_1 \left\{ f_1 + (\epsilon - \mu)\frac{\partial f_1}{\partial \epsilon} \right\} - \left\{ (\epsilon - \mu)\frac{\partial f_1}{\partial \epsilon} + \frac{1}{2}(\epsilon - \mu)^2 \frac{\partial^2 f_1}{\partial \epsilon^2} \right\}\right] + \cdots, \quad \text{(A39)}$$

where $f_1 = 1/(e^x \mp 1)$. We note that the $O(q-1)$ term of the generalized distribution in Eq. (65) derived by the OLM-MEM corresponds to the last term in the bracket of Eq. (A39).

APPENDIX B: SUPPLEMENT TO THE INTERPOLATION APPROXIMATION

1. Analytic expressions of q-FDD for $|\beta(\epsilon-\mu)| \ll 1$

We may obtain an expression of the q-FDD for small $x[=\beta(\epsilon-\mu)]$ with the use of an expansion for $f_1(\epsilon\beta)$ given by

$$f_1(\epsilon, \beta) = \frac{1}{2} + \sum_{n=1}^{\infty} d_{n,1} x^n \quad \text{for } |x| < 1. \quad \text{(B1)}$$

Substituting Eq. (B1) to Eqs. (76) and (77) and employing Eqs. (5) and (27), we obtain

$$f_q^{\mathrm{IA}}(\epsilon, \beta) = \frac{1}{2} + \sum_{n=1}^{\infty} d_{n,q} x^n \quad \text{for } |x| < 1, \quad \text{(B2)}$$

with

$$d_{n,q} = d_{n,1} \frac{(q-1)^n \Gamma\left(\frac{1}{q-1} + 1 + n\right)}{\Gamma\left(\frac{1}{q-1} + 1\right)} \quad \text{for } 1 < q < 3, \quad \text{(B3)}$$

$$d_{n,q} = d_{n,1} \frac{(1-q)^n \Gamma\left(\frac{q}{1-q} + 1\right)}{\Gamma\left(\frac{q}{1-q} + 1 - n\right)} \quad \text{for } 0 < q < 1, \quad \text{(B4)}$$

$$d_{n,q} = \begin{cases} q d_{n,1} & \text{for } n = 1, \quad \text{(B5)} \\ d_{n,q} = q(2q-1)d_{n,1} & \text{for } n = 2, \quad \text{(B6)} \\ d_{n,q} = q(2q-1)(3q-2)d_{n,1} & \text{for } n = 3, \quad \text{(B7)} \end{cases}$$

where $d_{n,1} = (1/n!)\partial^n f_1(\epsilon, \beta)/\partial x^n$ at $x=0$: $d_{1,1} = -1/4$, $d_{2,1} = 0$, $d_{3,1} = 1/48$, etc. Equations (B2)–(B7) lead to

$$f_q^{\mathrm{IA}}(\epsilon, \beta) \simeq \frac{1}{2} - \frac{q}{4}x + \frac{q(2q-1)(3q-2)}{48}x^3 + \cdots \quad \text{for } |x| < 1. \quad \text{(B8)}$$

2. Generalized Sommerfeld expansion in the IA

In the case of $q > 1.0$, Eq. (61) yields

$$\frac{\partial f_q(\epsilon)}{\partial \epsilon} = -\int_0^{\infty} G\left(u; \frac{q}{q-1}, \frac{1}{(q-1)\beta}\right) \frac{(\epsilon - \mu)e^{u(\epsilon-\mu)}}{[e^{u(\epsilon-\mu)} + 1]^2} du. \quad \text{(B9)}$$

Substituting Eq. (B9) to Eq. (109) and changing the order of integrations for ϵ and u, we obtain

$$c_{n,q} = \frac{\beta^n}{n!} \int_0^{\infty} G\left(u; \frac{q}{q-1}, \frac{1}{(q-1)\beta}\right) u^{-n} du \int \frac{x^n e^x}{(e^x + 1)^2} dx. \quad \text{(B10)}$$

At low temperatures, Eq. (B10) reduces to

$$c_{n,q} = \frac{2(1-2^{1-n})\zeta(n)}{(q-1)^n} \int_0^\infty G\left(u; \frac{q}{q-1}, 1\right) u^{-n} du, \quad \text{(B11)}$$

$$c_{n,q} = c_{n,1} \frac{\Gamma\left(\frac{1}{q-1} + 1 - n\right)}{(q-1)^n \Gamma\left(\frac{1}{q-1} + 1\right)} \quad \text{for even } n, \quad \text{(B12)}$$

$$c_{n,q} = 0 \quad \text{for odd } n. \quad \text{(B13)}$$

The ratio of $c_{n,q}/c_{n,1}$ is given by

$$\frac{c_{n,q}}{c_{n,1}} = \begin{cases} \dfrac{\Gamma\left(\frac{1}{q-1} + 1 - n\right)}{(q-1)^n \Gamma\left(\frac{1}{q-1} + 1\right)} & \text{for even } n, \quad \text{(B14)} \\ \dfrac{1}{2-q} & \text{for } n = 2, \quad \text{(B15)} \\ \dfrac{1}{(2-q)(3-2q)(4-3q)} & \text{for } n = 4. \quad \text{(B16)} \end{cases}$$

In the case of $q < 1.0$, Eqs. (62) and (109) yield

$$c_{n,q} = \frac{2(1-2^{1-n})\zeta(n)}{(1-q)^n} \frac{i}{2\pi} \int_C H\left(t; \frac{q}{1-q}, 1\right) (-t)^{-n} dt, \quad \text{(B17)}$$

$$c_{n,q} = c_{n,1} \frac{\Gamma\left(\frac{q}{1-q} + 1\right)}{(1-q)^n \Gamma\left(\frac{q}{1-q} + 1 + n\right)} \quad \text{for even } n, \quad \text{(B18)}$$

$$c_{n,q} = 0 \quad \text{for odd } n, \quad \text{(B19)}$$

leading to

$$\frac{c_{n,q}}{c_{n,1}} = \begin{cases} \dfrac{\Gamma\left(\frac{q}{1-q} + 1\right)}{(1-q)^n \Gamma\left(\frac{q}{1-q} + 1 + n\right)} & \text{for even } n, \quad \text{(B20)} \\ \dfrac{1}{2-q} & \text{for } n = 2, \quad \text{(B21)} \\ \dfrac{1}{(2-q)(3-2q)(4-3q)} & \text{for } n = 4. \quad \text{(B22)} \end{cases}$$

Equation (B20) for $q < 1.0$ is the same as Eq. (B14) for $q > 1.0$ if we employ the reflection formula of the gamma function,

$$\Gamma(z)\Gamma(1-z) = \frac{\pi}{\sin(\pi z)}.$$

3. Low-temperature phonon specific heat in the IA

In the case of $q > 1.0$, Eqs. (60) and (76) yield

$$C_q \simeq k_B \beta^2 \int_0^\infty G\left(u; \frac{q}{q-1}, 1\right) \times \int_0^\infty \frac{\rho(\omega)(q-1)(\hbar\omega)^2 u e^{(q-1)\beta\hbar\omega u}}{[e^{(q-1)\beta\hbar\omega u} - 1]^2} d\omega du$$

$$= \frac{9N_a k_B}{(q-1)^4} \left(\frac{T}{\Theta_D}\right)^3 \int_0^\infty G\left(u; \frac{q}{q-1}, 1\right) u^{-4} du \int_0^\infty \frac{x^4 e^x}{(e^x - 1)^2} dx \quad \text{(B23)}$$

$$= \alpha_q \left(\frac{T}{T_D}\right)^3, \quad \text{(B24)}$$

with

$$\alpha_q = \alpha_1 \frac{\Gamma\left(\frac{1}{q-1} - 3\right)}{(q-1)^4 \Gamma\left(\frac{q}{q-1}\right)} \quad \text{for } 1 < q < 3, \quad \text{(B25)}$$

where T_D $(=\hbar\omega_D/k_B)$ stands for the Debye temperature and α_1 is the T^3 coefficient of the low-temperature specific heat for $q = 1.0$.

In the case of $q < 1.0$, a similar analysis with the use of Eqs. (60) and (77) leads to

$$C_q \simeq k_B \beta^2 \left(\frac{i}{2\pi}\right) \int_C H\left(t; \frac{q}{1-q}, 1\right) \times \int_0^\infty \frac{\rho(\omega)(1-q)(\hbar\omega)^2 (-t) e^{-(1-q)\beta\hbar\omega t}}{[e^{-(1-q)\beta\hbar\omega t} - 1]^2} d\omega dt \quad \text{(B26)}$$

$$= \frac{9N_a k_B}{(1-q)^4} \left(\frac{T}{T_D}\right)^3 \left(\frac{i}{2\pi}\right) \int_C H\left(t; \frac{q}{1-q}, 1\right) \times (-t)^4 dt \int_0^\infty \frac{x^4 e^x}{(e^x - 1)^2} dx, \quad \text{(B27)}$$

from which we obtain

$$\alpha_q = \alpha_1 \frac{\Gamma\left(\frac{q}{1-q} + 1\right)}{(1-q)^4 \Gamma\left(\frac{q}{1-q} + 5\right)} \quad \text{for } 0 < q < 1. \quad \text{(B28)}$$

Equations (B16), (B22), (B25), and (B28) yield

$$\frac{\alpha_q}{\alpha_1} = \frac{1}{(2-q)(3-2q)(4-3q)} = \frac{c_{4,q}}{c_{4,1}} \quad \text{for } 0 < q < 4/3. \quad \text{(B29)}$$

[1] C. Tsallis, J. Stat. Phys. **52**, 479 (1988).
[2] C. Tsallis, Physica D **193**, 3 (2004).
[3] E. M. F. Curado and C. Tsallis, J. Phys. A **24**, L69 (1991).
[4] C. Tsallis, R. S. Mendes, and A. R. Plastino, Physica A **261**, 534 (1998).
[5] S. Martinez, F. Nicolas, F. Pennini, and A. Plastino, Physica A **286**, 489 (2000).
[6] G. L. Ferri, S. Martinez, and A. Plastino, J. Stat. Mech.: Theory Exp. **2005**, P04009.
[7] Lists of many applications of the nonextensive statistics are available at http://tsallis.cat.cbpf.br/biblio.htm.
[8] G. Wilk and Z. Wlodarczyk, Phys. Rev. Lett. **84**, 2770 (2000).
[9] C. Beck, Phys. Rev. Lett. **87**, 180601 (2001).
[10] C. Beck, in *Anomalous Transport: Foundations and Applications*, edited by R. Klages *et al.* (Wiley-VCH, New York, 2008), pp. 433–457.
[11] C. Tsallis and A. M. C. Souza, Phys. Rev. E **67**, 026106 (2003).
[12] A. K. Rajagopal, e-print arXiv:cond-mat/0608679.
[13] G. E. Crooks, Phys. Rev. E **75**, 041119 (2007).
[14] S. Abe, C. Beck, and E. G. D. Cohen, Phys. Rev. E **76**, 031102 (2007).
[15] E. Van der Straeten and C. Beck, Phys. Rev. E **78**, 051101 (2008).
[16] C. Beck, Europhys. Lett. **64**, 151 (2003).
[17] A. M. Reynolds, Phys. Rev. Lett. **91**, 084503 (2003).
[18] C. Beck, Phys. Rev. Lett. **98**, 064502 (2007).
[19] C. Beck, Physica A **331**, 173 (2004).
[20] M. Baiesi, M. Paczuski, and A. L. Stella, Phys. Rev. Lett. **96**, 051103 (2006).
[21] C. Tsallis, F. C. Sa Barreto, and E. D. Loh, Phys. Rev. E **52**, 1447 (1995).
[22] Diego F. Torres, Hector Vucetich, and A. Plastino, Phys. Rev. Lett. **79**, 1588 (1997); **80**, 3889(E) (1998).
[23] U. Tirnakli and D. F. Torres, Eur. Phys. J. B **14**, 691 (2000).
[24] F. Büyükilic, D. Demirhan, and A. Gülec, Phys. Lett. A **197**, 209 (1995).
[25] F. Pennini, A. Plastini, and A. R. Plastino, Phys. Lett. A **208**, 309 (1995).
[26] E. K. Lenzi, R. S. Mendes, L. R. da Silva, and L. C. Malacarne, Phys. Lett. A **289**, 44 (2001).
[27] Q. A. Wang and A. Lé Méhauté, Phys. Lett. A **235**, 222 (1997).
[28] U. Tirnakli, F. Büyükkilic, and D. Demirhan, Physica A **240**, 657 (1997).
[29] Q. A. Wang, Phys. Lett. A **242**, 301 (1998).
[30] F. Büyükilic, I. Sökmen, and D. Demirhan, Chaos, Solitons Fractals **13**, 749 (2002).
[31] U. Tirnakli and D. F. Torres, Physica A **268**, 225 (1999).
[32] M. E. Pessah, D. F. Torres, and H. Vucetich, Physica A **297**, 164 (2001).
[33] D. Torres and U. Tirnakli, Physica A **261**, 499 (1998).
[34] L. Salasnich, Int. J. Mod. Phys. B **14**, 405 (2000); **15**, 1253 (2001).
[35] K. S. Fa and E. K. Lenzi, Braz. J. Phys. **31**, 317 (2001).
[36] C. Ou and J. Chen, Phys. Lett. A **342**, 107 (2005).
[37] H. G. Miller, F. C. Khanna, R. Teshima, A. R. Plastino, and A. Plastino, Phys. Lett. A **359**, 357 (2006).
[38] S. Biswas, e-print arXiv:cond-mat/0606029; Phys. Lett. A **372**, 1574 (2008).
[39] A. Lawani, J. Le Meur, D. Tayurskii, A. El Kaabouchi, L. Nivanen, B. Minisini, F. Tsobnang, M. Pezeril, A. Le Méhaute, and Q. A. Wang, J. Low Temp. Phys. **150**, 605 (2008).
[40] I. S. Oliveira, Eur. Phys. J. B **14**, 43 (2000).
[41] L. H. M. Nunes and E. V. L. de Mello, Physica A **296**, 106 (2001); **305**, 340 (2002).
[42] H. Uys, H. G. Miller, and F. C. Khanna, Phys. Lett. A **289**, 264 (2001).
[43] M. Portesi, A. Plastino, and C. Tsallis, Phys. Rev. E **52**, R3317 (1995).
[44] F. D. Nobre and C. Tsallis, Philos. Mag. B **73**, 745 (1996).
[45] F. Buyukkilic, D. Demirhan, and U. Tirnakli, Physica A **238**, 285 (1997).
[46] M. S. Reis, J. P. Araújo, V. S. Amaral, E. K. Lenzi, and I. S. Oliveira, Phys. Rev. B **66**, 134417 (2002).
[47] M. S. Reis, V. S. Amaral, J. P. Araújo, and I. S. Oliveira, Phys. Rev. B **68**, 014404 (2003).
[48] M. S. Reis, V. S. Amaral, R. S. Sarthour, and I. S. Oliveira, Phys. Rev. B **73**, 092401 (2006).
[49] H. Hasegawa, Physica A **388**, 2781 (2009); **388**, 3675(E) (2009).
[50] A. K. Rajagopal, R. S. Mendes, and E. K. Lenzi, Phys. Rev. Lett. **80**, 3907 (1998).
[51] E. K. Lenzi, R. S. Mendes, and A. K. Rajagopal, Phys. Rev. E **59**, 1398 (1999).
[52] D. Prato, Phys. Lett. A **203**, 165 (1995).
[53] H. H. Aragao-Rego, D. J. Soares, L. S. Lucena, L. R. da Silva, E. K. Lenzi, and K. S. Fa, Physica A **317**, 199 (2003).
[54] M. R. C. Solis and J. P. H. Esguerra, e-print arXiv:0302094.
[55] S. Martinez, F. Pennini, A. Plastino, and M. Portesi, Physica A **332**, 230 (2004).
[56] E. K. Lenzi and R. S. Mendes, Phys. Lett. A **250**, 270 (1998).
[57] S. Martinez, F. Pennini, A. Plastino, and C. J. Tessone, Physica A **295**, 224 (2001); **309**, 85 (2002).
[58] P. G. Zamorano and F. A. U. Campos, Revista Mexicana De Fisica **53**, 198 (2007).
[59] T. Schmelzer and L. N. Trefethen, SIAM (Soc. Ind. Appl. Math.) J. Numer. Anal. **45**, 558 (2007).
[60] An application of the FA to nonextensive itinerant-electron (metallic) ferromagnets is inappropriate [49]. For example, (1) with decreasing q below unity, the Curie temperature calculated by the FA is *decreased* although the exact q-FDD yields *increased* T_C and (2) for $q>1.0$, a reduction in T_C calculated by the FA is much overestimated compared with that in the EA [61].
[61] H. Hasegawa, e-print arXiv:09060225.
[62] E. P. Borges, Physica A **340**, 95 (2004).
[63] T. Dauxois, S. Ruffo, E. Arimondo, and M. Wilkens, *Dynamics and Thermodynamics of Systems with Long Range Interactions*, Lecture Notes in Physics Vol. 602 (Springer, New York, 2002), p. 1.
[64] A. Lavagno and P. Quarati, Romanian Reports in Physics **59**, 951 (2007).
[65] M. Schmidt, R. Kusche, T. Hippler, J. Donges, W. Kronmuller, B. von Issendorff, and H. Haberland, Phys. Rev. Lett. **86**, 1191 (2001).
[66] H. Hasegawa, Physica A **351**, 273 (2005); Prog. Mater. Sci. **52**, 333 (2007).
[67] W. G. Unruh, Phys. Rev. D **14**, 870 (1976); **14**, 3251 (1976).
[68] W. Gordon, Ann. Phys. **377**, 421 (1923).